CHARACTERIZATION OF SURFACE SULFATE SPECIES ON MIXED METAL OXIDE CATALYSTS: INSIGHTS FROM SPECTROSCOPIC STUDIES

BY

SHREYAS ACHARYA

A thesis submitted to the

Graduate School-New Brunswick

Rutgers, The State University of New Jersey

in partial fulfillment of the requirements

for the degree of

Master of Science

Graduate Program in Chemical and Biochemical Engineering

Written under the direction of

Dr. George Tsilomelekis

and approved by

_____

_____

_____

New Brunswick, New Jersey

October, 2017

ABSTRACT OF THE THESIS

Characterization of surface sulfate species on mixed metal oxide catalysts: Insights from spectroscopic studies

by Shreyas Acharya

Thesis Director: Dr. George Tsilomelekis

Solid acid and super acid catalysts are promising alternatives for very important reactions usually catalyzed industrially by homogeneous acid reactions. Sulfated metal oxides are among many examples of solid super acids which work well for acid catalyzed reactions. These catalysts have applications in isomerization, alkylation, acylation and oxidative dehydrogenation reaction. A characteristic example encompasses products from tert-butylation of phenol which have tremendous importance in chemical, petrochemical as well as pharmaceutical industry. In spite of significant amount of work devoted in this area, the catalysts being commercially used have low yields. Hence we channel our efforts in enhancing the productivity of the alkylation of phenol reaction by using sulfated metal oxides as it has shown in our preliminary work improved catalytic activity. In this work, we focus on the preparation and characterization of sulfated mixed metal oxides. Specifically, sulfated-Tin-Zirconium oxides (STZ) are produced by coprecipitation method using hydrated Zirconium Oxychloride($ZrOCl_2.8H_2O$) and Tin Chloride($SnCl_4.5H_2O$) as metal precursors and ammonia as the precipitating agent. Different proportions of hydrous tin and zirconium oxides (molar ratios of 1:10,1:1 and 10:1) are synthesized. Sulfation of the prepared hydrous oxides is performed using wet impregnation method with 1M and 0.5M sulfuric acid solution. Calcination of the prepared sulfate mixed hydroxides follows at $600^{o}C$. Our work focuses on the incorporation of vibrational spectroscopic teqniques at the individual steps of the synthesis procedure. To that end, first we utilize Raman spectroscopy to study the

speciation of the metal salts precursors in water and at various pH range. The broad spectral envelope is assigned to specific vibational modes of the various species. XRD analysis is done to understand the crystalline phases of the catalyst. Additionally, we study the temperature evolution of the deposited sulfated species by means of in-situ Attenuated Total Reflection (ATR-FTIR) and in-situ Raman spectroscopy using high temperature reaction chamber. The results show that the molecular structure of the surface sulfate species varies significantly with increasing temperature as underscored by the changes of S=O vibrational bands. It was found that the sulfated species getting attached to the catalyst support can majorly be present as bidentate, tridentate and polymeric species and are a function of the temperature as well as the Sn:Zr ratio. Tuning the molecular structure of the sulfated species could potentially alter the acidic properties of the catalysts as indicated by the Lewis/Bronsted acid sites. Lastly, it was found that the crystalline phases of the the regenerated catalyst remain unaffected along with the sulfated groups.

ACKNOWLEDGEMENTS

CONTENTS

LIST OF TABLES

LIST OF FIGURES

1   INTRODUCTION

1.1   NATURE AND IMPORTANCE OF SOLID ACID CATALYSTS

Solid acids are heterogeneous materials with various acidic functional groups, often work as a heterogeneous catalyst. They are extensively used in oil and petrochemical industries with the motto of making the refining and production process economically and environmentally viable. Besides the petrochemical sector, the importance of solid acid catalysts in the chemical and pharmaceutical sector is unquestionable. Research on the synthesis and characterization of the solid acid catalysts is carried out heavily as its properties can be tuned by design.[1] The main factors governing the quality of solid acids are the Bronsted to Lewis acidity ratio, density and strength of acidic sites, pore size and its distribution and surface area. Tailoring the properties of the catalyst, for instance the strength of the acid, can help in improving the product selectivity. Moderately strong acid sites aid in hydrolysis and acetal reactions whereas isomerization (ex. n-butane to iso-butane isomerization), alkylation (ex.butylation of phenol) and esterification reactions require strong acid sites. Similarly, the nature of the acidic site plays a pivotal role. Lewis acids like aluminum chloride work well for Friedel Crafts alkylation of toluene with benzyl chloride whereas Brönsted acid sites give better results when benzyl alcohol is used as a reactant.[2]

Solid acid catalysts offer a wide range of advantages over homogeneous or liquid phase acid catalyzed reactions. Industries manufacturing ethane-1,2-diol from epoxyethane and Bisphenol A from phenol depend on mineral acids such as H_2SO_4, HF or Lewis acids like $AlCl_3$ and BF_3 for acid catalyzed reactions. These chemicals pose a threat to the environment as it generates large amounts of hazardous wastes. Treating these toxic wastes involves neutralization of the post-reaction mixture and hence making it very costly and complex processes. Taking into account the chloride ions involved and the nature of mineral acids, corrosion of reactors is a common issue. Lastly, liquid phase acid catalyzed reactions consist of energy intensive techniques for separation of product from the catalyst. All these issues can be overcome with the use of solid acid catalysts. Some of the types of solid acid catalyst are listed below.

Aluminumsilicates were the first solid acid catalyst used commercially for cracking process in petrochemical industries .[3] In the past, the pore size of amorphous silica alumina were controlled and greatly used for hydrocarbon conversions. Besides amorphous silica alumina catalyst, crystalline aluminasilicates, popularly known as zeolites, are currently used as solid acid materials. Zeolites are versatile catalysts which have replaced strong homogeneous acids, especially in the petrochemical sector. Replacement of Si^{4+} in zeolite framework to trivalent Al^{3+} induces bronsted acid sites. A heteropoly acid (ex. $H_3PW_{12}O_{40}$ Phosphotungstic acid or $H_3PMo_{12}O_{40}$ Phosphomolybdic acid) which can work as a homogeneous and heterogeneous catalyst are acids specifically made of hydrogen and oxygen along with metals such as tungsten, molybdenum or vanadium and non-metals such as silicon, phosphorous or arsenic.

Sulfated metal oxides is one of the examples of solid acid catalyst developed 35 years ago which established the idea that treatment of oxides of zirconium, tin, titanium, chromium, iron with sulfated groups can boost the surface area and acidity. The source of SO_4^{2-} on these metal oxides can be SO_2, H_2SO_4, $(NH_4)_2SO_4$, CS_2, H_2S. The presence of S=O on metal oxides generates acidic sites.[4] Sulfated metal oxides are used for reactions such as alkylation, isomerization, acylation etc. Representative sulfated and non-sulfated metal oxide solid acids along with their acidic strength [5] are shown below. (Table 1.1) Acid strengths have been estimated (Arataa and coworkers) by color change of Hammett indicator, TPD of pyridine, TPR of furan, and catalytic activity for various reactions.

Table 1.1:Solid super acids and their acidic strength

Catalyst	Calcination Temperature	Highest acid strength (Ho value)
SO4/SnO$_2$	550	-18
SO4/ZrO$_2$	650	-16.1
SO4/HfO$_2$	700	-16
SO4/TiO$_2$	525	-14.6
SO4/Al2O$_3$	650	-14.6
SO4/Fe$_2$O$_3$	500	-13
SO4/SiO$_2$	400	-12.2

WO3/ZrO$_2$	800	-14.6
MoO3/ZrO$_2$	800	-13.3
WO3/SnO$_2$	1000	-13.3
WO3/TiO$_2$	700	-13.1
WO3/Fe$_2$O$_3$	700	-12.5
B2O3/ZrO$_2$	650	-12.5

1.2   ZIRCONIA AS PROMISING CATALYST SUPPORT

Zirconia is one of the most universally used metal oxide catalyst mainly because of its ideal thermal and mechanical properties. It also offers good surface acidity and basicity, porosity and surface area[6] .

To synthesize zirconium oxide, Zirconyl chloride octahydrate (ZrOCl$_2$.8H$_2$O) is popularly used as a precursor salt. The zirconium ions exhibit a valency of +4 and it exists in the form of isolated polymeric tetramer cations $[Zr_4(OH)_8(H_2O)_{16}]^{8+}$ in aqueous solutions. This structure was confirmed using single crystal X-Ray analysis. It was concluded that zirconium is never bonded to chlorine either in aqueous solution or when it is in its oxide state.[7]

By dropping hydroxide base on aqueous solution of zirconium precursor salts, precipitation occurs which leads to the formation of hydrous zirconium oxides. The structural configurations and properties of zirconium oxides depend heavily on parameters such as the pH and aging time.[8-9] According to Clearfield, on the addition of hydroxyl base polymeric tetrameric zirconium species is formed. These species on calcination form a framework of zirconium oxides.[10]

Zirconia has four crystalline phases; namely, cubic, tetragonal, monoclinic, and orthorhombic. Orthorhombic phase is obtained only at high pressures. The monoclinic phase is stable at room temperature to about 1170 °C [11]. It has been reported that monoclinic zirconia shows better selectivity to butene in hydrogenation of carbon monoxide reactions[12] and works as a better support than tetragonal zirconia in production of methanol from carbon monoxide[13].

The tetragonal phase is stable above 1170 ºC and below the cubic range temperature of about 2370 ºC. At low temperatures a metastable tetragonal phase is obtained by sulfating amorphous zirconium oxide followed by calcination. According to the surface

energy effects, at lower temperatures, tetragonal phase of zirconia is stabilized when the particle size is less than or equal to around 30nm.[14] Sulfation of zirconia leads to reduction in the particle size as it decelerates the oxo-zirconium bonds. Sulfation overcomes sintering issues and hence prevents phase transformation.[15]

The application of sulfated zirconia as an acid catalyst was introduced for the first time when it proved to be effective for the isomerization of n-butane at moderate temperatures.[16] Tetragonal zirconia shows better selectivity towards methane, ethene, propene during the hydrogenation of carbon monoxide reactions and higher activity in n-butane isomerization reactions.[12, 17-18]

1.3   TIN OXIDES AS STRONG ACID CATALYST SUPPORT

Tin dioxides (SnO_2) are used as catalysts, gas sensors, transistors etc. It exhibits dual valency exists in 2+ or 4+ oxidation state[19]. This dual valency property develops alteration in the constitution of surface oxygen and thud helps in tuning the surface properties. This greatly helps in tailoring the catalyst according to the desired strength and density of acid sites. SnO_2 is popularly known as 'cassiterite' in its mineral form. Tin oxides are generally used as an oxidative catalyst in the production of carboxylic acids and acid anhydrides from aromatic compounds.

  Sulfating the tin oxide catalyst has helped to improve its surface area and its surface acidity which in turn has enhanced its catalytic activity. Temperature-programmed reactions of adsorbed furan [20] have shown SO_4^{2-}/SnO_2 to be one of the strongest solid acids. Sulfated tin has been reported as the most efficient catalyst for alkylation of hydroquinone. [21]

1.4   WHY MIXED METAL OXIDES SHOULD BE USED?

  Sulfated Zirconia undergoes deactivation on reduction or after reaction at high temperatures. To avoid this problem, zirconia is doped or stabilized with other metal oxides that lead to sulfated mixed metal oxide. It has been reported that these types of oxides have better stability and increased acidity compared to the transition metal impregnated on the sulfated zirconia catalyst[22-25]. The acidity of the mixed oxides is

believed to be resulting from the excess of negative or positive charges caused by the bridged hetero metal–oxygen bonds (M-O-M').[26] It is observed that the doping of zirconia with Al, Fe, Si and Mn ions helps in stabilizing the tetragonal phase, improving the surface area and sulfate uptake[27-28]. There have been very limited research efforts on the doping of zirconia with tin oxide and hence synthesizing sulfated tin zirconium oxide and characterizing them will give better insights and understanding of its application as a catalyst.

1.5 SYNTHESIS METHOD

Co-precipitation is the synthesis method used in this project. It is a simple technique used to obtain consistency, with respect to the amounts of precursor salts, in the composition of catalyst. Aging, pH, solution composition, anions, temperature, precipitating agent are the factors which affect the morphology, textural properties, purity etc. Hence optimizing these parameters to obtain the desired material is of prime importance. A pH of 8 has been selected for precipitating the metal hydroxide because the solubility of Zirconium ion species increases at a pH>8. Also, the particle size of metal hydroxides decreases with increase in pH. It is also observed that the higher concentration of precursor salt before precipitation, the larger the particle size of precipitate.

The concentration of sulfuric acid during wet impregnation may have an impact in the sulfate species deposited on the metal oxide and also influence the Lewis to Brönsted acid ratios to a great extent. It has been reported that the overall acidity of sulfated zirconia is highest when impregnated with 0.5M H_2SO_4. The following progression in the acidities were reported for sulfated zirconia(SZ).[29]

Brønsted acidity : SZ [0.5M] >> SZ [1M] > SZ [0.25M];

Lewis acidity : SZ [0.5M] > SZ [1M] > SZ [0.25M];

Total acidity : SZ [0.5M] >> SZ [1M] > SZ [0.25M].

In this work, the mixed metal oxides are treated with 1M and 0.5M sulfuric acid and the variations in sulfated species depending on the concentration are studied.

Calcination process which is essentially a heat treatment process is carried out to remove or decompose counterions into volatile products and convert the amorphous materials into crystalline materials. The order of calcination in the synthesis process of sulfated metal oxides also plays an important role. Apart from Al_2O_3, acidic sites were

not effectively generated by the treatment of sulfates on the crystallized oxides of iron, titanium, zirconium, hafnium and tin. However they were produced when the amorphous hydroxide were treated with sulfate groups followed by calcination.[30]

1.6   VIBRATIONAL SPECTROSCOPY

Vibrational Spectroscopy collectively consists of Infrared Spectroscopy and Raman Spectroscopy. Both these analytical techniques are heavily used for structure elucidation, material characterization, functional group identification, qualitative and quantitative analysis. IR spectroscopy is an absorbance phenomenon whereas Raman Spectroscopy is a scattering phenomenon. Both these techniques give complementary information and in unison these techniques are informative tool for structure elucidation which is the strong focus of this research. IR spectroscopy is governed by change in the dipole moment whereas Raman spectroscopy is governed by change in polarizability. Information about both these techniques has been elaborated below.

The stretching frequency of a bond can be approximated by Hooke's law.

$$v = \frac{1}{2\pi}\sqrt{\frac{k}{\mu}}$$

Here v is the vibrational frequency,k is the force constant and μ is the reduced mass. Hence higher the force constan k, higher energy is required to excite the molecule, leading to a vibrational band at higher frequency, vice versa for reduced mass.

1.6.1   IR SPECTROSCOPY

IR spectroscopy uses infrared radiations as a source and measures the quantity of incident radiations absorbed by the sample. Infrared spectrum is a molecular vibrational spectrum. When the sample is excited with infrared radiation, specific wavelengths which are characteristic to the molecule are selectively absorbed. This enables the change of dipole moment. The vibrational mode will be IR active only when there is a change in dipole moment.

Consider the CO_2 molecule. Carbon dioxide is a linear molecule and hence the number of vibrational modes will be (3N-5, where 'N' is number if atoms) 4. For a non-linear

molecule e.g. water, the number of vibrational modes is given by 3N-6. The 4 vibrational modes of carbon dioxide are shown in the Figure 1.1

Figure 1.1: Vibrational modes of Carbon dioxide
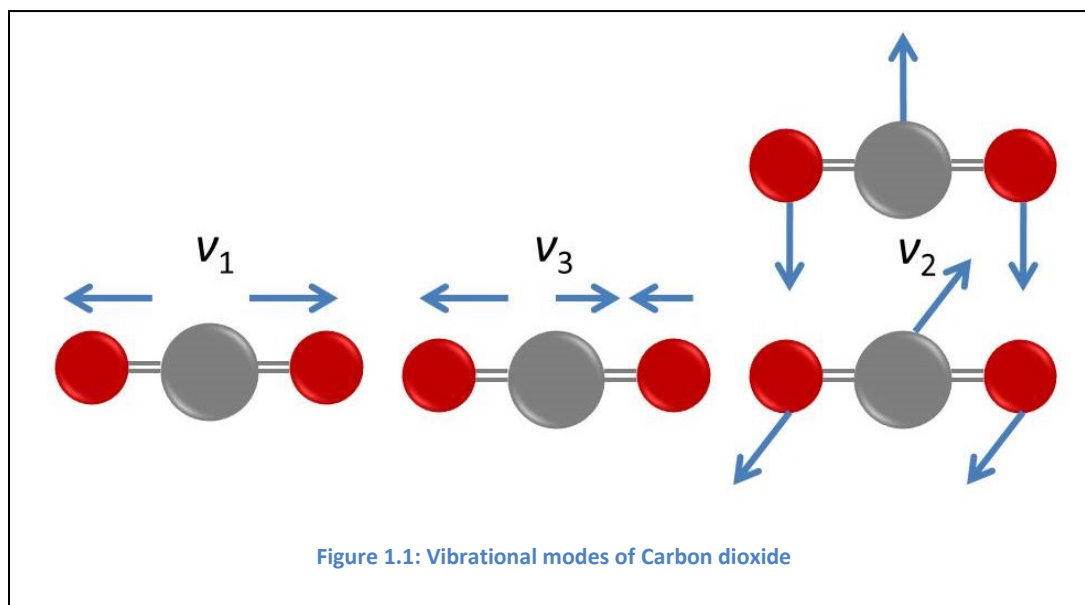
- v_1 : symmetric stretching mode (elongation and contraction of bond in phase)
- v_3 : asymmetric stretching mode (elongation and contraction of bond out of phase);
- v_2 : 2 different types of bending modes.

The symmetric stretching band is generally seen at a lower wavenumber than asymmetric stretching because the energy required to excite the molecule to symmetric stretching iscomparatively less. Also symmetric stretching for linear molecule doesn't change the dipole moment but for non-linear molecules such as water the dipole moment increases when the O-H bond stretching occurs and decreases when bond contracts. Hence for molecules like water the vibration is IR active. Diatomic molecules (O_2, N_2 and Cl_2) are IR inactive. IR spectroscopy scans the sample from 400-4000cm^{-1}. FTIR spectroscopy results into a spectrum after computing a series of wavelengths which are used to excite the sample.

The spectroscopic data obtained through the FTIR in this research is by using Attenuated total reflectance (ATR) unit which is an accessory to the FTIR instrument.

The diamond crystal is the heart of the ATR unit and depending upon its refractive index the total reflectance is governed. Diamond, ZnSe, Germanium are high refractive index crystals which are generally used in ATR unit.

The incident IR beam gets reflected into the tube several times and generates evanescent beam which comes into contact with the sample, the reflected beam is then collected by the detector.

1.6.2 RAMAN SPECTROSCOPY

Raman spectroscopy is an inelastic scattering of light phenomenon. UV, Visible light or near Infrared is used as a source in Raman spectroscopy because it has higher energy than IR, leading to excitation at higher excitation states. This helps to avoid absorption of photons. When the molecules lose energy to return to ground state or lower excitation state, scattering reactions occur. The 3 types of scattering are:

- Rayleigh scattering: Occurs when the light is elastically scattered i.e scattered light has the same energy as the incident light
- Stokes scattering: Occurs when the scattered light settles at a higher energy state (First excited vibrational level) than its previous energy state.
- Anti-Stokes scattering: Occurs when the scattered light it loses energy during this process and the system reaches a lower energy level than its previous energy state

Rayleigh and Raman are two photon processes involving scattering of incident light. The incident photon is absorbed transiently, and then a new photon is formed when transition occurs from ground state into a virtual state. Rayleigh scattering is the most probable event compared to Raman scattering. Change in polarizability makes the Raman scattering active. The polarizability is a measure for the electron cloud's ability to deform in contrast to the atomic nuclei. The change of the polarizablity depends on the molecule geometry.

1.7 PROPOSED CONFIGURATIONS OF SULFATED SPECIES

The sulfated species developed on the catalyst support play an important role in a modulating the Lewis to Bronsted acid ratio. Hence understanding the type and molecular structure of the surface sulfated species is of utmost importance. The relative

concentration of metal oxides can be influential in modulating the surface dispersed species as individual metal oxides vary in its oxidation states and its ionic radii. The molecular structure (see Figure 1.2) of sulfated species on metal oxide was introduced by Yamaguchi and co-workers for the first time, where they hypothesized that the surface had Lewis sites exclusively. [31] The structure is a covalent chelating bidentate sulfate structure and was observed in iron oxides (Fe_2O_3).
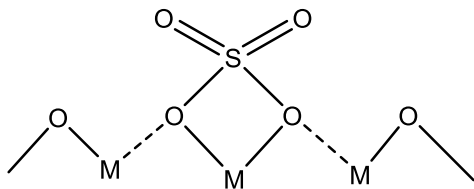
Figure 1.2: Proposed structure of chelating bidentate sulfated group on metal oxide

The possibility of existence of bridged bidentate sulfate species (a sulfate species whose 2 out of 4 oxygen atoms are connected to the metal atom) was also put up by Yamaguchi and his co-workers. The structure is shown below in Figure 1.3
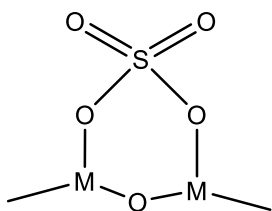
Figure 1.3: Proposed structure of bridged bidentate sulfated group on metal oxides

Yamaguchi and coworkers compared the structural configuration of the surface sulfates formed on the metal oxides with organic sulfates. The surface sulfate acquires high covalency which is fairly equivalent to the organic sulfonates and sulfates. They assigned the bands at 1240-1230, 1125-1090, 1035-995, 960-940 cm^{-1} to chelating bidentate sulfate structure exhibiting. The chelating and bridged bidentate sulfate species is denoted as '**β**' in all the spectra.

They pointed out the theory that distinguishing factor between chelating and bidentate sulfate species is that the extreme frequency vibrational band of chelating is higher than the highest frequency vibrational band of bridged sulfate species.[32] The concept of band splitting with decrease in symmetry is addressed in the next paragraph.

The free sulfate ion belongs to T_d symmetry and only one broad band at 1100cm^{-1} is observed. The triple degeneracy of the band leads to one band with exception of a band at 975 cm^{-1} in few cases. The symmetry gets lowered when the sulfate group forms complex with metal ions resulting to C_{3v} symmetry for monodentate complex. The asymmetric *(v₃)* vibrational band splits into two, one at 975cm^{-1} and the other at higher wavenumber. For bridged bidentate sulfate configuration the symmetry becomes C_{2v}, and bands become visible at 1000, 1050 and around 1200-1220 cm^{-1}. When the structural configuration of bidentate species takes the chelating form, the highest asymmetric vibrational frequency is observed at higher frequency (around $1250 < v < 1300$cm-1) as that of bridged configuration. This concept is explained pictorially below.
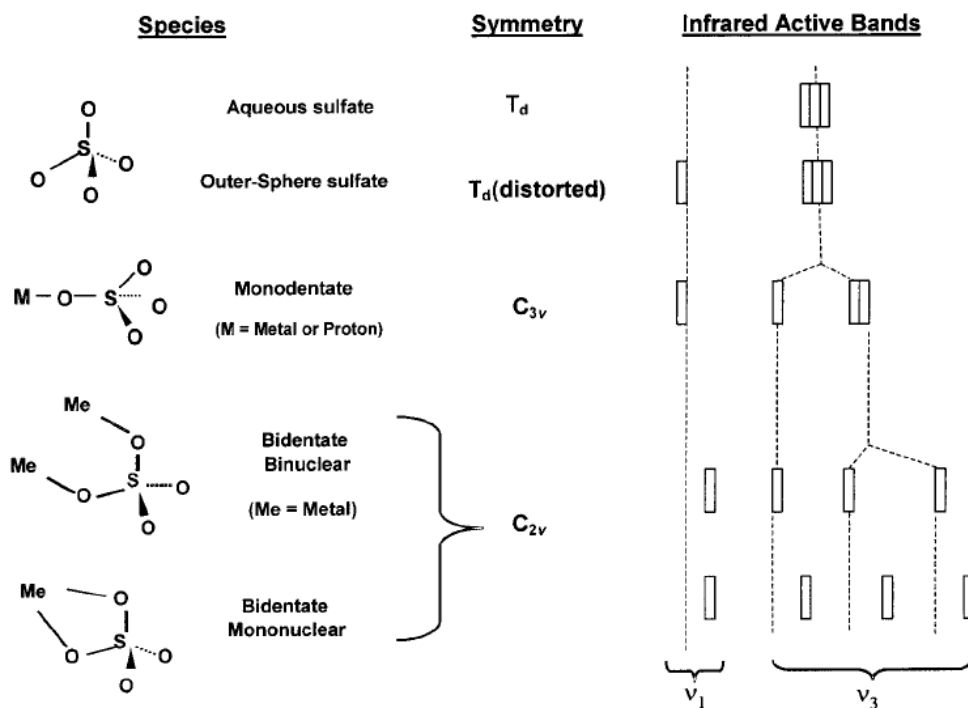
Figure 1.4: IR spectrum bands to distinguish between chelating and bridged bidentate sulfate complexes. Adapted from Hug [33]

In order to take into account the Brønsted acid sites, a structure shown in Figure 1.5 is a proposed model of sulfated group on zirconia by Ward et.al.[34]. It is a modified structure which is also a chelating bidentate sulfate structure. Mortera et al. studied the behavior of

sulfated zirconia by injecting H_2O vapors and observed two broad bands at 1130 and 1280cm^{-1}, which was typical of bidentate sulfato complex.[35]
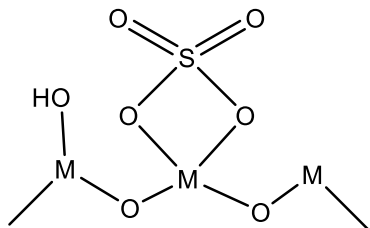
Figure 1.5: Proposed structure of modified chelating bidentate sulfated group on metal oxides
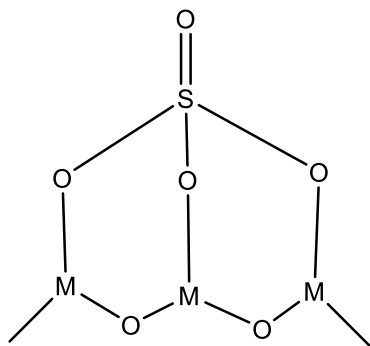
Figure 1.6: Proposed structure of tridentate sulfated group by Bensitel and co-workers

The Figure 1.6 is the structure which was first introduced by Bensitel and co-workers.[36-37] It consists of single S=O structure and the rest includes three oxygen atoms bonded to the metal component by single bonds. When the sulfate group was increased significantly they suggested the possibility of existence of one more sulfate species. This structure is indicated in Figure 1.7.
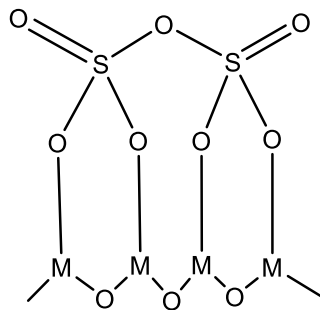
Figure 1.7: Proposed structure of polymeric sulfate group on metal oxides by Lavalley and co workers

The tridentate species is represented as 'τ' whereas polymeric sulfate species are represented as 'ρ' in the spectra compiled in the results and discussion section. Bensitel and coworkers used different types of sulfating source and postulated that the all these sources lead to same types of surface sulfate species at dehydrated conditions. According to their interpretation from the IR spectra, the sulfate structure exhibits 2 type of species, both with single S=O oscillator. The difference in these species is believed to be due to anchoring of these sulfate species on different crystalline faces of zirconia. They used isotopic exchange of oxygen at high temperatures to propose the tridentate species with single S=O oscillator. It was also concluded that these sulfate species were free from any kind of hydrogenosulfate species using heavy water (deuterium) for hydration. This research group assigned the peaks arising at 1370, 1355, 1035, 968, 947, 930cm^{-1} to tridentate species. They also hypothesized the existence of polysulfate S_2O_7 species at high temperature loadings displaying bands at 1004, 1085 and 1400cm^{-1}. Riemer and coworkers[38] came to an agreement to the above work by making use of Raman spectroscopy and NMR.

It was further reported that the effect due to hydration on these metal oxides influences the structure of sulfated groups to a large extent. They speculated that the structure of sulfated group on hydration will have more of ionic character and it will be attached to only 2 metal atoms. The hypothesized structure is shown below in Figure 1.8
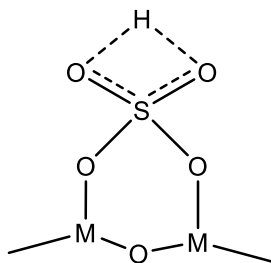
Figure 1.8: Proposed structure of hydrated sulfated group on metal oxides.

Through ab initio calculations Hasse and Sauer showed that the bidentate structures are not thermodynamically stable at high temperatures and get converted to tridentate species. They predicted the spectral splitting for tridentate species between vibrational bands of S=O and S-O to be 350cm^{-1} whereas for bidentate species the spectral splitting of S=O symmetric and asymmetric stretching to be 90cm^{-1}.[39]

A different structure of sulfated zirconia with 5-coordination surface atoms was proposed by White et al. [40]. Each sulfur atom in this structure is surrounded by five oxygen atoms (see Figure 1.9.)
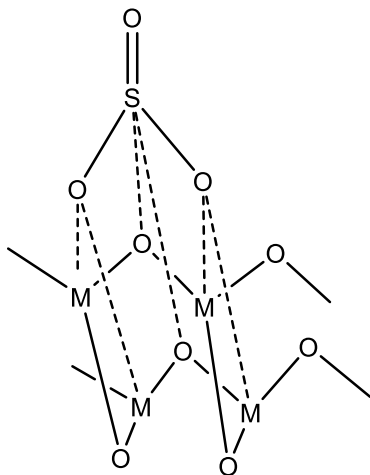
Figure 1.9: Proposed structure of sulfated group on metal oxides by white et. al.

1.8 BUTYLATION OF PHENOL

The tert-butylation reaction of phenol has tremendous commercial value. The major products of this reaction are 2,4-di-tert-butylphenol (2,4-DTBP), 4-tert-butylphenol (4-TBP) and 2-tert-Butylphenol (2-TBP). 2,4-DTBP is a raw-material used in the manufacture of stabilizers for PVC or UV absorbers in polyolefins.[41] It is a primal matter for producing antioxidants as well. 4-TBP plays a crucial role in the production of phenol formaldehyde resins. These resins are used as surface coatings binders or varnishes. 2-TBP is used as a feedstock in the production of antioxidants and agrochemicals. As mentioned earlier, reaction temperature and nature of acid sites are the two main factors which govern the selectivity of these products. In this research we have restricted our reaction condition to only 150°C. Nature of acid sites varies as the amount of tin doping is altered. In order to elaborate on the importance of nature of acid sites on the selectivity of products some of the examples are given below.

1. Zeolite-Y is a weak solid acid when used as a catalyst with phenol and tert-butanol, leads t-butyl phenyl ether (t-BPE).

2. H-BEA considered to be a strong acid catalyst showed enhanced selectivity for m-t-butylphenol (m-t-BP)[42].

3. Moderate acid catalysts tend to favor products such as o-t- and p-t-butylphenol (o-t-BP and p-t-BP)[43]

4. Sulfated zirconia favors p-t-butylphenol with the improved activity only when alkylating agent used is in higher proportions. [44]

5. Sulfated tin oxide shows poor activity for butylation of phenol reaction but it has proved to be the most efficient catalyst for the alkylation of hydroquinone.[21]

As per our knowledge, sulfated zirconium and tin mixed oxides haven't been used for these reactions. Determining the nature of acid sites is beyond the scope of this project but depending on the conversion and selectivity it is possible to draw an idea about the nature of the catalyst synthesized.

1.9   GIST OF THIS WORK

In this work, mixed metal oxide of zirconium and tin is produced and its crystalline structures are compared with sulfated mixed metal oxide of zirconium and tin. There is limited understanding and ambiguity in the structure of sulfate species developed on zirconia and tin oxides. Therefore an attempt to decipher the type of sulfate species developed depending on the composition of the mixed metal oxide and the condition of the catalyst (hydrated or dehydrated) is made. The materials produced are used as catalyst for butylation of phenol which was part of the research we undertook in this thesis. The long term goal of this project is to develop an efficient catalyst for the alkylation of phenol and also to determine if there is any relationship or reliance of the selectivity of the products on the type of sulfate species developed. The following chapters are dedicated to the synthesis and characterization of sulfated zirconium-tin oxides. The 4th chapter will help to draw insights about the sulfate species using vibrational spectroscopy. In order to analyze the applicability of the generated material as a catalyst, the catalytic activity and regeneration ability of some of the catalyst is also covered in this project.

2 EXPERIMENTAL SECTION

2.1 CHEMICAL REAGENTS

Reagents for catalyst synthesis

Zirconium oxychloride (Zirconyl chloride octahydrate) $ZrOCl_2.8H_2O$ is in the form of white powder and is water soluble chloride salt of zirconium. Zirconium oxychloride [Molecular weight 322.25, CAS No.7699-43-6, Sigma-Aldrich 98% reagent grade, 100gm] is used as zirconium source for the synthesis of the catalyst.

Tin(IV) chloride pentahydrate $SnCl_4.5H_2O$ [Molecular weight 350.6, CAS No. 10026-06-9, Sigma-Aldrich 98% reagent grade, 100gm] is in the form of solid lumps which is water soluble and is used as the precursor for synthesis of zirconium tin hydroxide .

Aqueous ammonia solution (Ammonium hydroxide) [Sigma-Aldrich, 28-30 wt%, 2.5L] is a colorless liquid used as a precipitating agent for the co-precipitation of zirconium and tin salts in its respective hydroxide forms.

Concentrated sulfuric acid (conc. H_2SO_4) [Sigma-Aldrich, 5M, 1L], is a colorless solution used for the wet impregnation of mixed metal hydroxides with sulfated groups

Reagents for Alkylation Reaction

Phenol [Molecular weight 94.11, CAS no. 108-95-2, Alfa Aesar 99.5% unstabilized, 100gm] is of solid melt form and is used as one of the reactants for the alkylation reaction.

Tert-butyl alcohol [molecular weight 74.12, CAS no. 75-65-0, Fisher Chemical, reagent grade, 99.5%] is a colorless liquid which has a boiling point of 83ºC and is used as an alkylating agent in the reaction carried out in a parr reactor.

2.2   CATALYST SYNTHESIS

The mixed hydroxides of zirconium and tin were prepared by the co-precipitation method and described next:

Dissolving in water

Firstly, both the precursor salts were separately dissolved in water. The concentration of the salts in its aqueous solutions was always maintained to 0.1M. These solutions were stirred in 2 separate beakers with magnetic stirrers. In order to synthesize mixed oxide catalysts, these separately dissolved salts were then mixed together. This mixture was later kept for proper mixing for half an hour.

Co-precipitation

A pH meter was used to continuously monitor the pH of the solution. The pH meter probe [Cole-Parmer pH electrode, Electrode type: Double junction, Electrode body material: Epoxy, gel filled] was immersed in the beaker containing the above mixture. The simultaneous precipitation of more than one component is called as co-precipitation. See Figure 2.1.

This solution containing $ZrOCl_2.8H_2O$ (0.1M) and $SnCl_4.5H_2O$ (0.1M) was
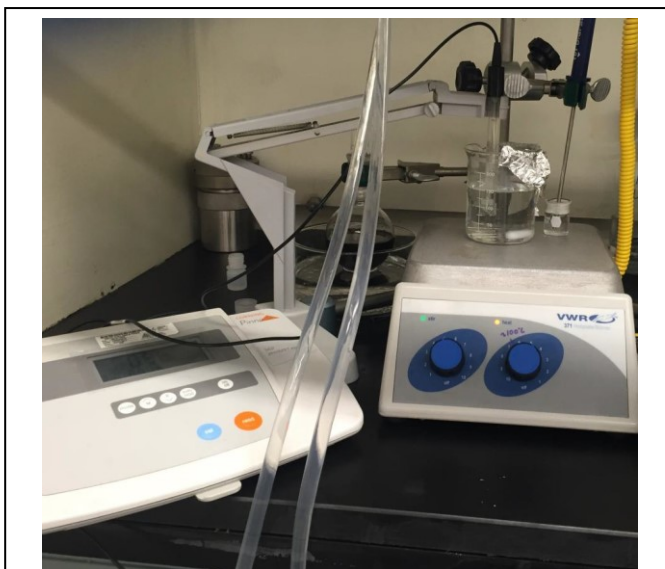
Figure 2.1: Experimental setup for the co-precipitation process

hydrolyzed with ammonia solution by drop wise addition and was vigorously stirred until the pH 8 was reached. At this pH hydroxides of both components i.e. Zirconium and Tin gets co-precipitated. A white precipitate is observed and is allowed to age for an hour. The obtained precipitate was filtered and washed thoroughly with deionized water to ensure the chloride ions do not get incorporated with the hydroxides. Fisherbrand glass fiber filter circles G6 were used for filtration process. These offer higher retention

efficiency of fine particles (<3μm in size). The filtered solid is kept for drying in the vacuum oven overnight at 85°C.

The product obtained after drying the filtered solids are hydrous tin–zirconium oxides. Half of the amount of hydrous tin–zirconium oxides was sent for calcination to form crystalline mixed oxides.

Figure 2.2: Vaccum oven used for drying

Wet Impregnation

Wet impregnation was carried out on the remaining amount of hydrous oxides, where they were stirred with 1M and 0.5M sulfuric acid for 1 hour. The excess was filtered off and the filtered solids were kept in the vacuum oven overnight at 85°C.

Calcination

The oven-dried sulfated hydrous tin-zirconium hydroxides were calcined for 3 hours at 600°C or 500°C (only

Figure 2.3: Experimental setup for sulfation of hydrous mixed oxides using wet impregnation process.

sulfated and non-sulfated hydrous tin oxides) with a ramp rate of 5K/min in the presence of air flow of 100ml/min.

Figure 2.4: Experimental setup and image of Calcination furnace [Lindeberg Blue M] from Thermo scientific
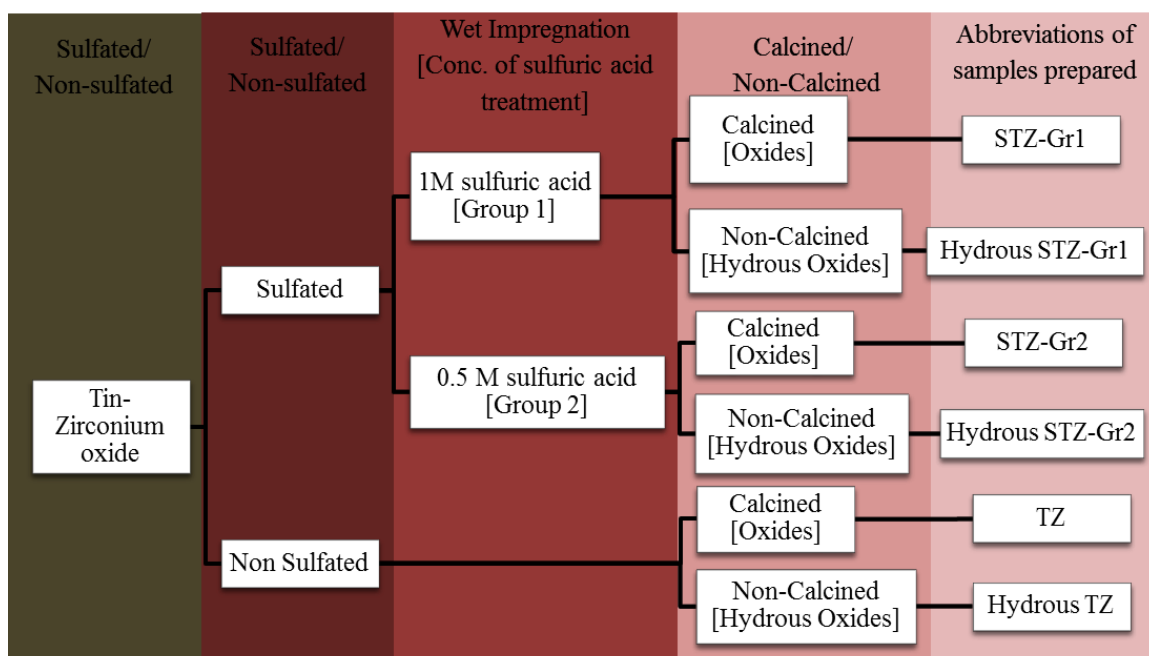
Figure 2.5: Overview of the materials generated over the synthesis process

Proportions of tin and zirconium in the catalyst prepared

The proportions of a component (for ex. Zirconium or Tin) in the mixed oxide used during co-precipitation process and the concentration of sulfuric acid used during wet impregnation process are tabulated in Table 2.1 and Table 2.2 respectively. The following abbreviations are used to represent specific metal or mixed metal oxides.

'T' signifies Tin oxide, 'Z' represents Zirconia, 'TZ' represents Tin-Zirconium mixed metal oxides with different molar ratios. Similarly for Sulfated metal oxides and mixed metal oxides 'ST' Sulfated Tin oxide, 'SZ' represents Sulfated Zirconia, 'STZ' represents Sulfated Tin-Zirconium mixed metal oxides

Table 2.1: Various proportions of mixed metal oxides produced

Material	Tin-Zirconium molar ratio	Calcination temperature
T (tin oxide)	[1:0]	500°C
TZ (tin-zirconium oxide)	[10:1]	600°C
TZ (tin-zirconium oxide)	[1:1]	600°C
TZ (tin-zirconium oxide)	[1:10]	600°C
TZ (tin-zirconium oxide)	[1:25]	600°C
Z (zirconium oxide)	[0:1]	600°C

Table 2.2: Various proportions of sulfated mixed metal oxides produced.

Material	Tin-Zirconium molar ratio	Calcination temperature	Concentration of Sulfuric acid used	
			Group 1	Group 2
ST (Sulfated tin oxide)	[1:0]	500°C	1M	0.5M
STZ (Sulfated tin-zirconium oxide)	[10:1]	600°C	1M	0.5M
STZ (Sulfated tin-zirconium oxide)	[1:1]	600°C	1M	0.5M
STZ (Sulfated tin-zirconium oxide)	[1:10]	600°C	1M	0.5M
STZ (Sulfated tin-zirconium oxide)	[1:25]	600°C	1M	-
SZ (Sulfated zirconium oxide)	[0:1]	600°C	1M	0.5M

2.3   BUTYLATION OF PHENOL REACTION

To test the activity of the materials produced, 1:1 STZ Group 2 and 1:10 Group 2 catalyst were used for the butylation of phenol. These reactions were carried out in a 25ml Parr reactor at atmospheric pressure and temperature of 150ºC for a reaction time of 7 hrs. The weight ratio of the reactant to alkylating agent was kept as 1:2 and the catalyst weight utilized was around 13% of the amount of phenol used. The quantitative analysis of the product and the reactant was done using GC-MS.
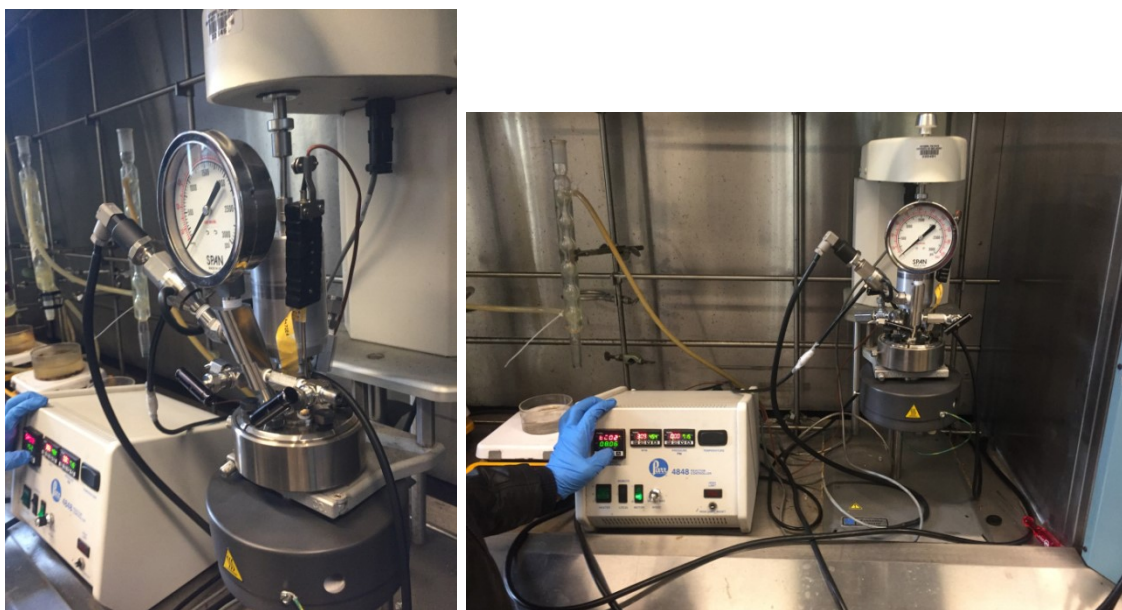
Figure 2.6:Experimental setup for alkylation of phenol reaction

CHAPTER 3

3   CATALYST CHARACTERIZATION

3.1   RAMAN SPECTROSCOPY

Raman spectra were recorded using Horiba UV-NIR LabRAM HR Evolution Raman spectrometer. It is a high spatial and spectral resolution Raman spectrometer equipped with a confocal microscope. It is equipped with an air cooled open electrode 1024x256 pixels CCD -75°C and a laser source of 532nm. The additional feature is the UV-Vis-NIR macro lens of 40 mm focal length for open geometry Raman configuration. Raman Spectrometer was used to characterize the hydrous TZ, TZ, hydrous STZ-Gr1, hydrous STZ Gr-2, STZ-Gr1, STZ-Gr2 materials. The spectra were recorded in dark room to avoid interference of light. Laser-safety goggles were used whenever Raman spectrometer was in use. The 10x objective was used for focusing the laser on the samples. Images are captured using the microscope (See Figure 3.1)
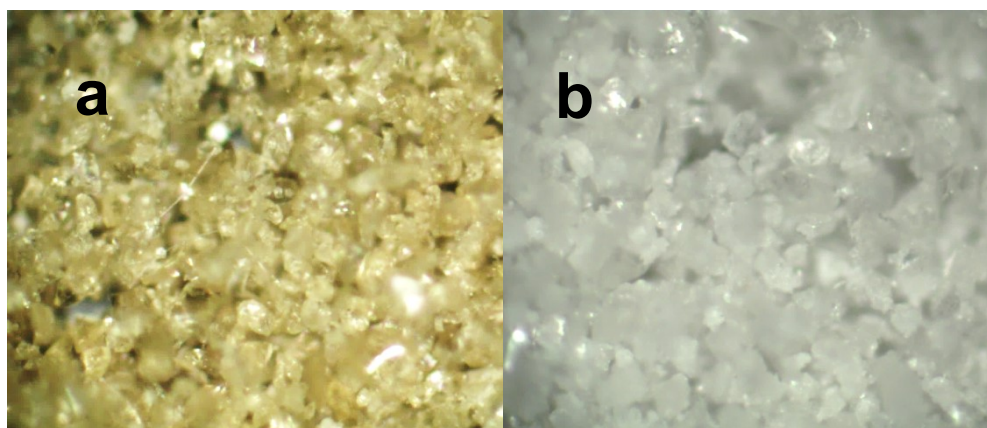
Figure 3.1:Magnified images of (a)SO_4^{2-}/SnO_2, (b)SO_4^{2-}/ZrO_2 using 10x objective of spectrometer

To get very high resolution spectra of the sulfated groups (900-1450cm^{-1}) the 100x objective was used. Images are captured using the microscope. The parameters were regulated using the LabSpec software.

Table 3.1: Values of parameters used in Raman Spectrometer

Parameters	Value
Acquisition time	75sec or 150sec(for sulfated groups)

Accumulations	10
Wavenumber range	50-1700cm^{-1}
Objective	x10 or x100(for sulfated groups)
Laser Intensity	10%
Grating	1800
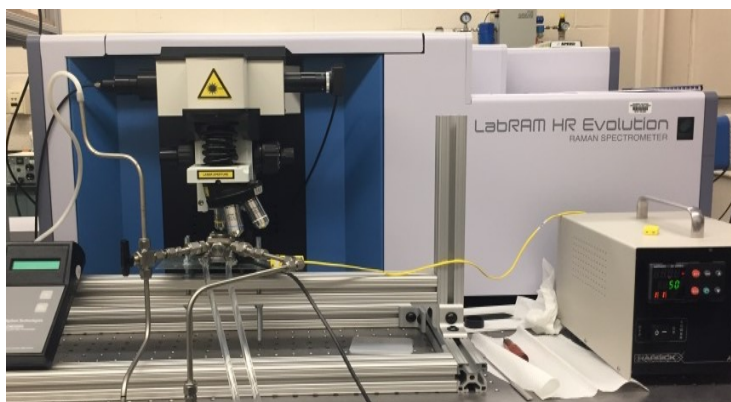
Figure 3.2: HORIBA LabRAM HR Evolution Raman Spectrometer

3.1.1   HIGH TEMPERATURE REACTION CHAMBER

Raman spectra of calcined catalyst at high temperatures were taken using a high temperature reaction chamber (HVC). Chilled water was constantly circulated into the HVC and the catalyst was dehydrated at high temperatures. During this process the catalyst was kept in an oxidizing environment by continuously flowing air. The spectra were taken at temperatures up to 500°C. The spectra were taken after stabilizing the catalyst at a particular temperature for 1 hr. See Figure 3.3 for HVC
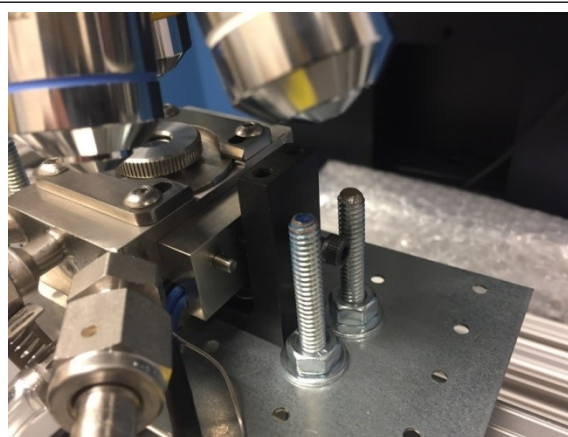
Figure 3.3: High Temperature Reaction Chamber

3.2   FOURIER TRANSFORM INFRARED SPECTROMETER-ATTENUATED TOTAL REFLECTANCE (FTIR- ATR)

FTIR spectra were collected using NICOLET IS50 FT-IR spectrometer. This analytical instrument is a high resolution (~0.9 cm-1) infrared spectrometer and is equipped with DLaTGS and MCT-A detectors. For this research project only DLaTGS detector was used. It contains long lifetime Polaris™ infrared source and gold optics. The FTIR is connected to a Parker-Balston 75-45 purge unit to provide a purified purge gas and air bearing gas from compressed air. The purge gas generator supplies carbon dioxide free air. This helps in obtaining cleaner background spectra in a shorter period of time and more accurate analysis by improving the signal-to-noise ratio. All the samples mentioned in the flowchart are characterized using FTIR at room temperature. Attenuated Total Reflectance technology is incorporated with this FTIR. The FTIR-ATR is used to characterize the type of sulfated species developed on the tin-zirconium oxide support.

Figure 3.4:Thermo Scientific NICOLET IS50 FTIR spectrometer

Specac ATR is a high-performance single reflection monolithic diamond ATR. One of the characteristic features of this equipment is that it can analyze a wide range of materials irrespective of the material's abrasiveness, hardness, reactivity or corrosiveness. The ATR platform is connected with an electrical heating unit which enables the platform to reach a maximum temperature of 300°C. With the help of this heating unit the STZ-Gr1 and STZ-Gr2 catalyst are characterized at higher temperatures as well. The changes in the sulfated species with respect to temperature are recorded at 25, 50, 100, 150 and 200°C. To get high resolution peaks of the sulfated groups the parameters of FTIR were selected accordingly using OMNIC software.

Table 3.2: Values of parameters used in FTIR-ATR

Parameters	
Detector	DTGS
Beam Splitter	KBr
Resolution	$4cm^{-1}$
Wavenumber range	$400\text{-}4000cm^{-1}$
Aperture	100
No.of scans	128
Optical Velocity	0.1581cm/sec

Figure 3.5:Specac ATR

3.3 X-RAY DIFFRACTOMETER

XRD data was collected to draw insights about the crystal phase and structures of the TZ, STZ-Gr1, STZ-Gr2 catalyst. The XRD equipment used here has a Cu anode and a PHILIPS PW1710 Goniometer. It is also equipped with a mini proportional counter detector, graphite monochromator, programmable receiving slit, 15-sample changer; sample spinner.

Table 3.3: Values of parameters used in XRD

Parameters	Value
K-Alpha1 wavelength	1.540598
K-Alpha2 wavelength	1.544426
Ratio K-Alpha2/K-Alpha1	0.5
Receiving slit	0.2
Generator voltage	45Kv
Tube current	40Ma
Scan range	$20^{o}\text{-}93^{o}$
Scan step size	0.02
No. of points	3650
Time per step	$2^{o}/min$
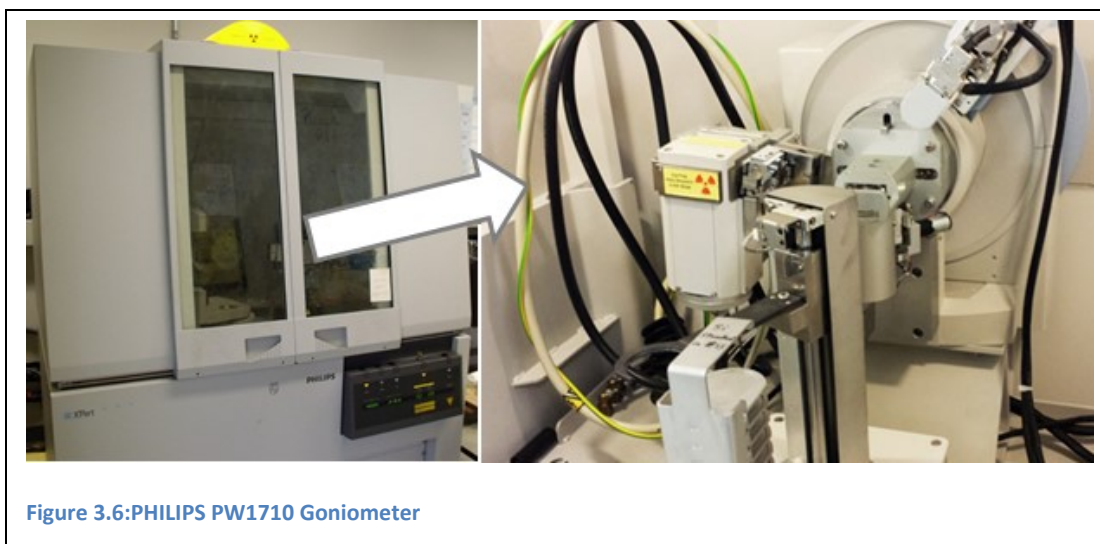
Figure 3.6:PHILIPS PW1710 Goniometer

3.4 NITROGEN ADSORPTION ISOTHERM METHOD FOR SURFACE AREA DETERMINATION

Qauntachrome Autosorb –I was used for determining the specific surface area of the samples. Before calculating the BET surface area of the STZ-Gr2 and TZ catalyst the samples were outgassed for 3 hrs at 300°C. The BET measurements were collected at 77 K in the liquid nitrogen bath. The Quantachrome Autosorb-I uses physical adsorption and capillary condensation
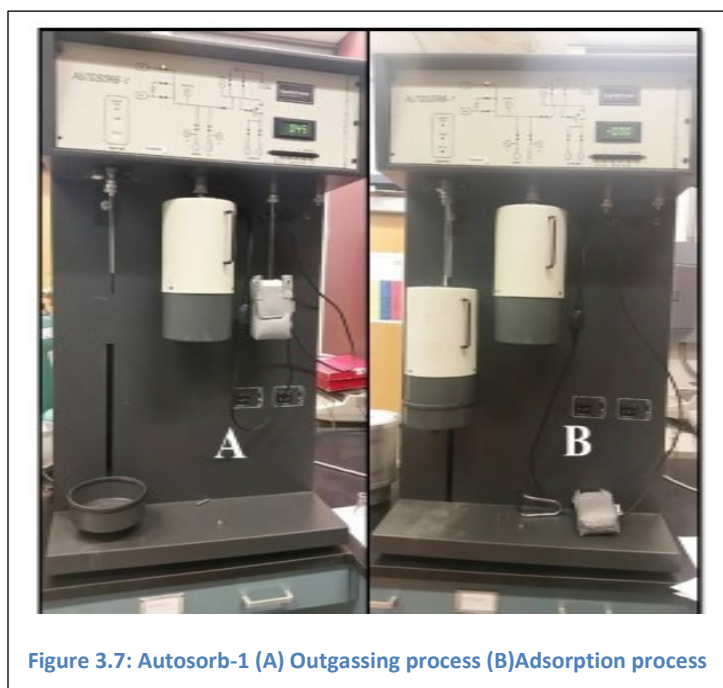
Figure 3.7: Autosorb-1 (A) Outgassing process (B)Adsorption process

principles to obtain information about the surface area and porosity of a solid material. It can measure surface areas as low as 0.005m^2/g using nitrogen as the adsorbate.

CHAPTER 4

4 RESULTS AND DISCUSSIONS

4.1 CATALYST TEXTURAL PROPERTIES

The values of the BET surface areas of the catalysts synthesized can be seen in Table 4.1. The BET surface area measurement is carried out only on the materials which are impregnated with 0.5M sulfuric acid. The crystalline phases of the synthesized materials are determined using Raman Spectrscopy and XRD. The BET surface areas of sulfated metal oxides/ Sulfated Mixed metal oxides show higher values with respect to its corresponding non sulfated metal or mixed oxides. This is verified from the literature. The values of Sulfated Zirconia and Sulfated tin oxides are comparable with the literature values as shown in Table 4.1. Sulfated metal oxides show higher surface area because sulfate species prevent the particles from sintering and hence reducing the particle size which in turn increases the surface area.

Table 4.1: Catalyst crystalline phases and Surface Areas

Material	Temp. ^{o}C	Color	Conc. H_2SO_4	Crystalline Phase	S.A. m^2/g	Values m^2/g
T	500	Y	-	Tetragonal Tin oxide	43	30.5[45]
ST	500	Y	1M	Tetragonal Tin oxide	-	66-
			0.5M	Tetragonal Tin oxide	91	93[45-46]
10:1 TZ	600	Y	-	Tetragonal Tin oxide	34	*37.4[47]
10:1 STZ	600	Y	1M	Tetragonal Tin oxide	-	
			0.5M	Tetragonal Tin oxide	81	
1:1 TZ	600	L. Y.		Monoclinic[1] + Tetragonal[2]	54	*31.4[47]
1:1 STZ	600	L. Y	1M	Monoclinic[1] + Tetragonal[2]	-	
			0.5M	Monoclinic[1] + Tetragonal[2]	74	
1:10 TZ	600	W		Monoclinic Zirconia	55	*35.8[47]
1:10 STZ	600	W	1M	Tetragonal Zirconia	-	53[48]
			0.5M	Tetragonal Zirconia	129	

		W		Monoclinic Zirconia	45	30-40[29, 48]
Z	600					
		W	1M	Tetragonal Zirconia	-	90-
SZ	600		0.5M	Tetragonal Zirconia	149	150[29, 34, 49]

[1] denotes Monoclinic phase of only Zirconia,

[2] denotes Tetragonal phases of both Zirconia+ Tetragonal Tin Oxide.

*The catalyst was calcined at 650 ^{o}C in the above stated reference's research work

Y:Yellow, W:White, L. Y: Light Yellow, S.A. denotes Surface area

4.2   METAL OXIDES AND MIXED METAL OXIDES

RAMAN SPECTRA
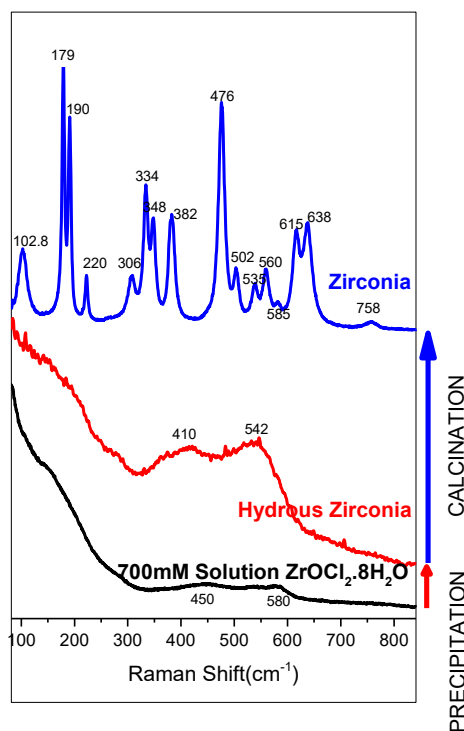
Figure 4.1: Raman Spectra of aqueous solution of Zirconium oxychloride, hydrous zirconia and Zirconia
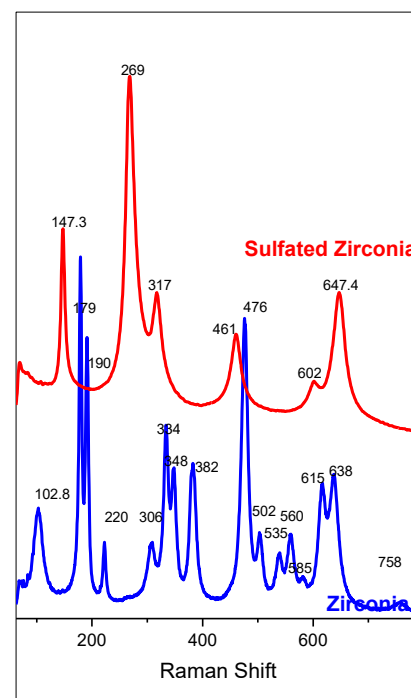
Figure 4.2: Raman Spectra of Zirconia and Sulfated Zirconia

Figure 4.1 shows the change in the Raman spectra of aqueous solution of the precursor salt, Zirconyl chloride Octahydrate, hydrous Zirconia and Zirconia. The aqueous

solutions show two major bands for pure Zirconyl chloride solution. One at 450cm^{-1} and the other at 580cm^{-1}. These bands can be assigned to Zr-O vibrations within the bridging hydroxyl groups. [50-51] The band at 450 cm^{-1} is typical of the cyclic tetramer ($[Zr_4(OH)_8(H_2O)_{16}]^{8+}$) defined below. Furthermore, more condensed species are also detectable from the bands at 430cm^{-1} and 540 cm^{-1} which would correspond to the presence of stacks of cyclic tetramers into the solution[52-53]. These two bands are assigned to Zr-O vibration within the bridging hydroxy groups between two zirconium atoms

  Generally the vibrations of metal-oxygen single bonds lie in the 200-850-cm^{-1} region. The Zirconyl chloride solution, hydrous zirconium oxides have two principle bands in this region. By comparing the Raman spectra for precursor solutions and the hydrous oxides a significant shift or replacement was noticed. For hydrous zirconium oxide, a band was observed at 540cm^{-1}. The 580^{-1} and 540 cm^{-1} bands, in the precursor solution and the hydrous oxides spectra respectively, belong to the same vibration. The band shifts because of polymerization process.   On calcination, the hydrous zirconium oxide (amorphous) turns into crystalline zirconium oxide and hence distinctive peaks of zirconium oxide can be observed in Figure 4.2. The bands of zirconium oxide (see Table 4.2) are assigned in the Figure 4.1 and it is attributed to the monoclinic phase[54]. Monoclinic phase of zirconium oxide exists after calcination at temperature as high as 600°C.[55]

Table 4.2: Raman shifts and symmetry of monoclinic zirconia

This work (cm^{-1})	102.8	179	190	220	306	334	348	382	476	502	535	560	615	638
Ishigame et. al[56] (cm^{-1})	102	179	190	222	305	334	348	381	476	500	534	556	615	637
Symmetry modes	Ag	Ag+ Bg	Ag	Bg	Ag	Bg	Ag	Bg	Ag	Bg	Bg	Ag	Bg	Ag

By comparing the Raman Spectra of sulfated zirconia and zirconia, it is concluded that zirconium oxides directly exhibit monoclinic phase whereas sulfated zirconia show tetragonal phase after calcination at 600°C. These results coroborate with the XRD spectra described later. Sulfation of hydrous zirconium oxide prevens the direct

transformation of amorphous phase to monoclinic phase. Generally sulfation leads to increase in surface area of the metal oxides, which is supported by the BET surface area measurement experiments addressed in the result and discussion section. Increase in surface area can imply that there is reduction in particle size. According to the surface energy effects, tetragonal phase of zirconia is stabilized when the particle size is less than or equal to around 30nm.[14] The bands of sulfated zirconia in Figure 4.2 are attributed to the tetragonal phase of zirconia.

Table 4.3: Raman Shifts and symmetry of tetragonal zirconia

This work (cm^{-1})	147.3	269	317	461	602	647.4
Naumeka et. al[57] (cm^{-1})	152	265	321	468	610	646
Symmetry modes	$E^+_{3\alpha}$	$E^+_{2\alpha}$	$(B_1^+)_1$	$(B_1^+)_2$	$E^+_{1\alpha}$	A_1^+

Figure 4.3 shows the Raman spectra of aqueous solution of tin(IV)chloride, hydrous tin oxide and tin oxide. A major band at $331 cm^{-1}$ in aqueous solution spectrum can be attributed to the $Sn(OH)_6^{2-}$ complex. Precipitating tin oxides out form its aqueous solution leads to significant changes. The bands appearing at higher wavenumbers may be due to the hydration effect and can be attributed to the Sn-O vibrational modes. On precipitation disappearance of the band at $331 cm^{-1}$ and appearance of a peak at $434 cm^{-1}$ can be noticed.

Figure 4.3:Raman Spectra of aqueous solution of tin chloride, hydrous tin oxide and tin oxide
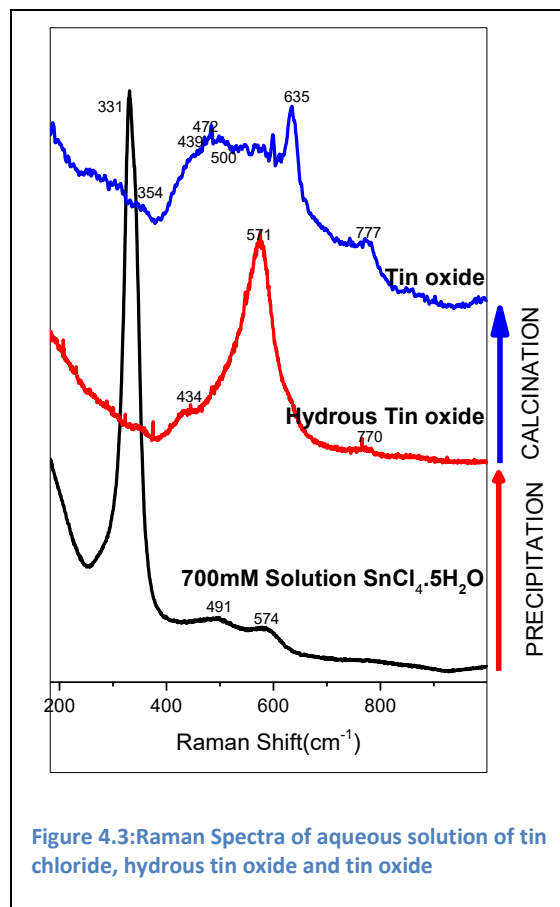
The Raman spectrum of the calcined tin oxide reveals that it has a tetragonal rutile structure. XRD spectra described later also support this result.

Table 4.4: Raman Shifts and Symmetry of tin oxide

	T(^{o}C) calcination	A$_{1g}$	B$_{2g}$	E$_g$	S$_1$	S$_2$
This work	500	635	777	479	569	502
Dieguez et al.[58]	450	635.2	774.2	479.7	568.9	493.2

Table 4.4 consists of major bands observed after calcination. The obtained spectral bands match well with the data presented in the literature.[58] The bands at 635cm^{-1},777cm^{-1} and 439cm^{-1} belong to classic vibrational modes but the bands represented by S1 and S2 symmetry modes are the surface related modes. According to Dieguez et al. these bands arise mainly due to disordered crystal configurations which hinders the in phase vibrations and thus obstructing their displacements to be verified. The disordered layer forms a shell like structure to the crystalline core and this surface layer of SnOx could lead to evolution of bands S$_1$ and S$_2$. The reason for this specificity of tin oxides to form surface layers could be due to the high reactivity of tin oxide with oxygen or any ambient gas.

In this study, we are using tin oxide as the second component of mixed metal oxide with zirconia. Tin has multivalency [Tin (IV) and Tin (II)] which can help in tuning the Lewis to Bronsted acidity ratio.

Raman Spectra of aqueous solutions of precursor salts

In Figure 4.4 the Raman spectra of aqueous solution of the mixture precursor salts are stacked up together. The 1:1 Zr:Sn and 9:1 Zr:Sn represent the molar ratios of Zirconyl chloride (ZrOCl$_2$.8H$_2$O) and Tin Chloride (SnCl$_4$.8H$_2$O) used in the mixture. The remaining two spectra, as mentioned in the Figure 4.4, denote pure aqueous solution of precursor salts. The Raman spectra of the aqueous solution were taken to understand the differences between the bands appearing in the spectra of aqueous solution and the hydrous oxides obtained after co-precipitation. This helps in discerning the species of the

salts taking part during precipitation and also to understand the behavior in which spectrum varies when the solutions are mixed with different proportions. As mentioned earlier, the bands at 450 and 580cm^{-1} in the pure $ZrOCl_2.8H_2O$ spectra belong to Zr-O vibrations within the bridging hydroxyl groups. When tin chloride (9:1-Zr:Sn) is added a distinctive peak at 331 starts appearing which is attributed to the $Sn(OH)_6^{2-}$ complex. The peaks at 450 and 580cm^{-1} can still be noticed. When the tin content is increased to equimolar ratios there is a drastic increase in intensity of the band at 331 cm^{-1} and bands at 491 and 574 cm^{-1} can be seen. As

Figure 4.4: Raman Spectra of aqueous solution of precursor salt
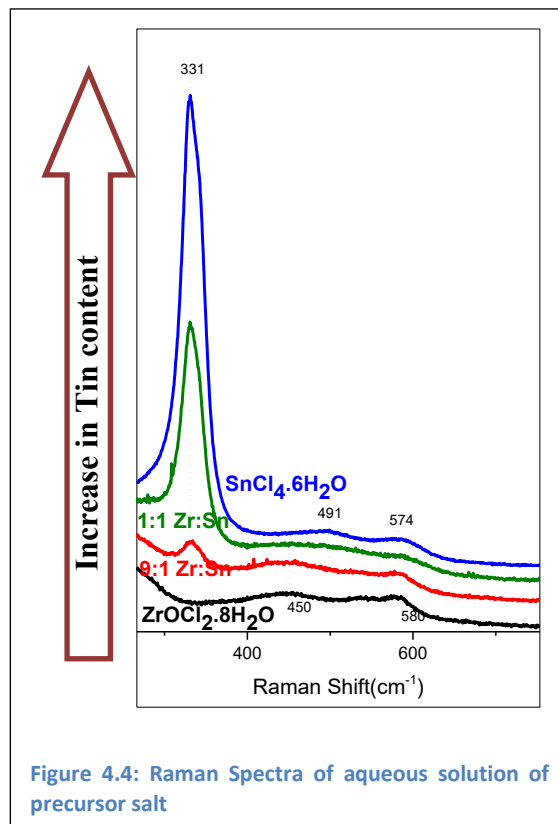
discussed earlier for Figure 4.3 both these bands represent Sn-O vibrational modes, which means that the signals of zirconium complexes in the Raman spectra get overshadowed by tin complexes even though mixture contains equimolar ratios of both salts. The peaks at 580 for zirconium salts and bands at 574 cm^{-1} for tin salts get shifted to lower wavenumbers when precipitated out. This signifies that the same species vibrate at lower wavenumbers when its state changes.

Raman Spectra of hydrous mixed oxides

Figure 4.5 is a compilation of the Raman Spectra of all the hydrous mixed metal oxides synthesized. The spectra of hydrous mixed oxides at Raman shifts from 100-800 denote metal oxide bonds and no conspicuous shifts can be observed even after sulfating these hydrous oxides. Hence the Raman spectra of sulfated hydroxides are not included in this report. The Raman spectra for hydrous zirconium oxide and hydrous tin oxide have already been discussed. All the varying proportions denoted in the Figure 4.5 denote molar ratios of the respective precursor salts used in the mixture. For example hydrous

1:25 TZ represents hydrous 1:25 Tin-Zirconium oxide where for every 1 mole of $SnCl_4.6H_2O$ 25 moles of $ZrOCl_2.8H_2O$ is added to the mixture. These hydrous oxides obtained after co-precipitation and drying overnight at 85°C, exhibit broad metal oxygen bands. This is because of its amorphous nature and hence the Raman scattering is poor. The spectra are very similar when the hydrous 1:25 TZ spectrum is compared with hydrous Zirconium (hydrous Z) spectrum. When the tin content is increased to 1:10 TZ, the band originally at $542cm^{-1}$ (represents Zr-O vibration
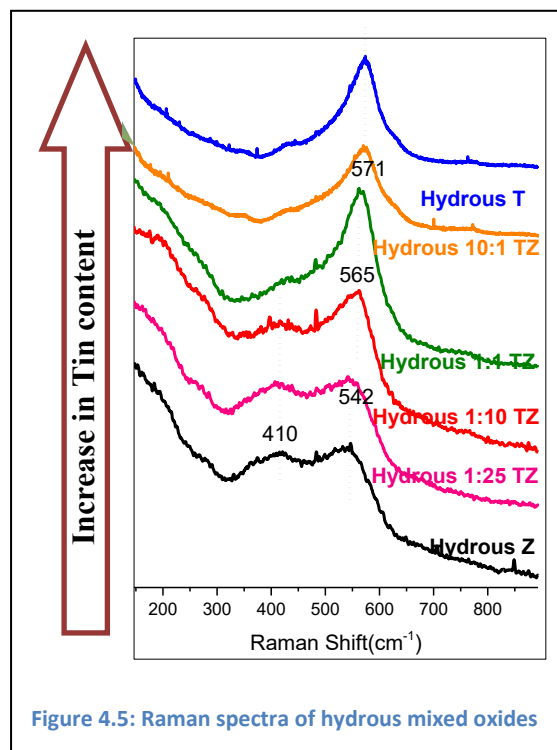
Figure 4.5: Raman spectra of hydrous mixed oxides

within the bridging hydroxyl groups between two zirconium atoms) shifts to $565cm^{-1}$. This blue shift is due to of the significant amount of tin addition. The $565cm^{-1}$ band can be attributed to a combination of Zr-O and Sn-O vibration within the bridging hydroxyl groups between Zirconium and tin atoms. Further increasing the tin content to hydrous 1:1 TZ, the spectra remains the same but there is an increase in the intensity of band at $565 \ cm^{-1}$ due to convolution of increasing Sn-O bands with Zr-O bands. At higher proportions of tin, 10:1 TZ and T, the signals of Zr-O vibrations get overshadowed and a broad peak can be observed at $571cm^{-1}$ which is attributed to Sn-O vibrational mode.

Raman Spectra of Mixed metal oxides and Sulfated mixed metal oxides

Figure 4.6 and Figure 4.7consists of Raman spectra of all the mixed metal oxides and sulfated mixed metal oxide catalyst respectively, synthesized with different proportions of tin and zirconium. We have chosen to show herein the sulfated mixed metal oxide spectra which are impregnated with 1M sulfuric acid (Gr 1); the spectra of sulfated mixed metal oxides impregnated with 0.5M sulfuric acid (Gr 2) show no differences. As reviewed earlier Figure 4.2 and Figure 4.1, zirconia and sulfated zirconia (in Figure 4.6 and Figure 4.7) show two different crystalline phases. Zirconia exhibits monoclinic phase whereas sulfated zirconia exhibits tetragonal phase. Similarly, the spectra of 1:25 TZ and

1:10 TZ are extremely identical to Raman spectra of zirconia suggesting that minute proportions of tin doping does not affect the crystal phase of zirconia. Also, the Raman spectra of 1:25 STZ and 1:10 STZ are identical to sulfated zirconia. Although distinct bands of tin oxide cannot be seen for Raman spectra of 1:25 TZ, 1:10 TZ, 1:25 STZ and 1:10 STZ, the width of the bands can be seen increasing when doped with tin. This can be attributed to defects in crystallites. The absence of tin oxide bands in zirconia rich oxides can be due to two reasons:

- Raman scattering is poor for cases such as Tin oxides.
- Tin oxides are present in a highly dispersed state in zirconia framework. This

Figure 4.6: Raman Spectra of mixed metal oxides

Figure 4.7: Raman Spectra of sulfated mixed metal
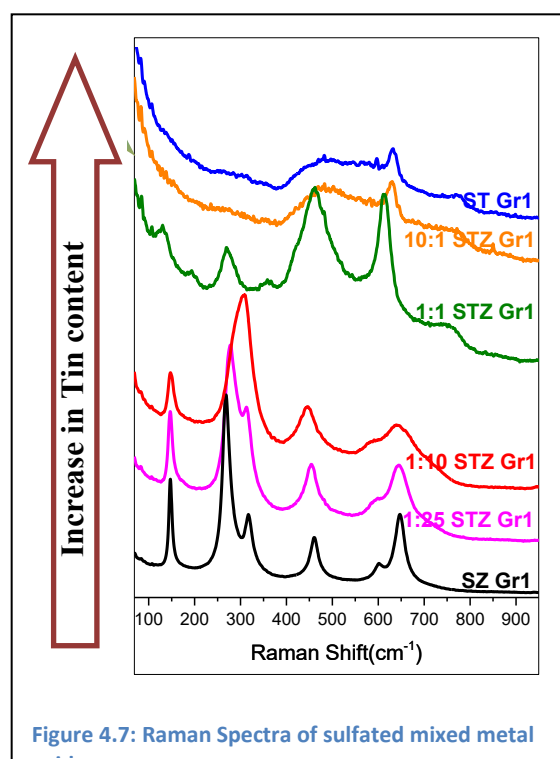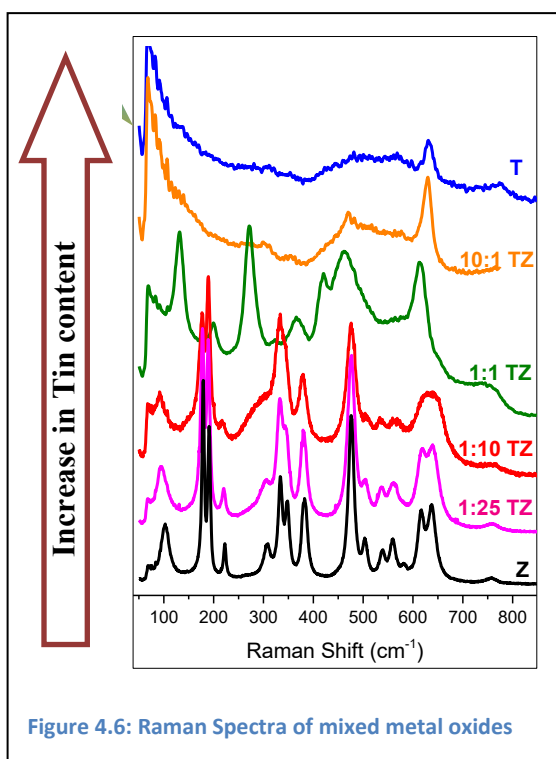
dispersed state prevents the generation of explicit crystalline tin oxide phase. As the Raman scattering is poor for tin oxides, very few distinctive bands of crystalline tin oxides can be seen. The tin rich oxides i.e. 10:1 TZ, T, 10:1 STZ and ST illustrate similarity in their Raman spectra and hence it can be implied that all these 4 materials show tetragonal tin oxide phase. The sulfated tin rich oxides have broader bands compared to non-sulfated tin oxides; this may result due to the smaller particle size of sulfated oxides.

The Raman spectra of 1:1 TZ is neither completely similar to monoclinic zirconia nor is it completely identical to tetragonal zirconia. At equivalent molar ratios of tin and zirconium, even without sulfation, some tetragonal phase coexists with monoclinic phase. The Raman spectra of 1:1 STZ matches fairly with the Raman spectra of 1:1 TZ (see Figure 4.8). The only distinct difference between these spectra is the appearance of the band at 419 cm^{-1} in 1:1 TZ spectra which appears as a shoulder in 1:1STZ Raman spectra. This can be due to sulfation effect as it reduces the particle size. A broad peak at 750 cm^{-1} units? can be a convoluted peak of monoclinic phase of zirconia and a peak of tetragonal phase of tin oxide. The high intensity bands at 269 cm^{-1} and 460 cm^{-1} representing $E^{+}_{2\alpha}$ and $(B_1^{+})_2$ symmetry modes of tetragonal phase of zirconia can be seen matching with the bands at 272 cm^{-1} and 460 cm^{-1}. This suggests that both these types of oxides exhibit more of tetragonal crystal phase characteristics.
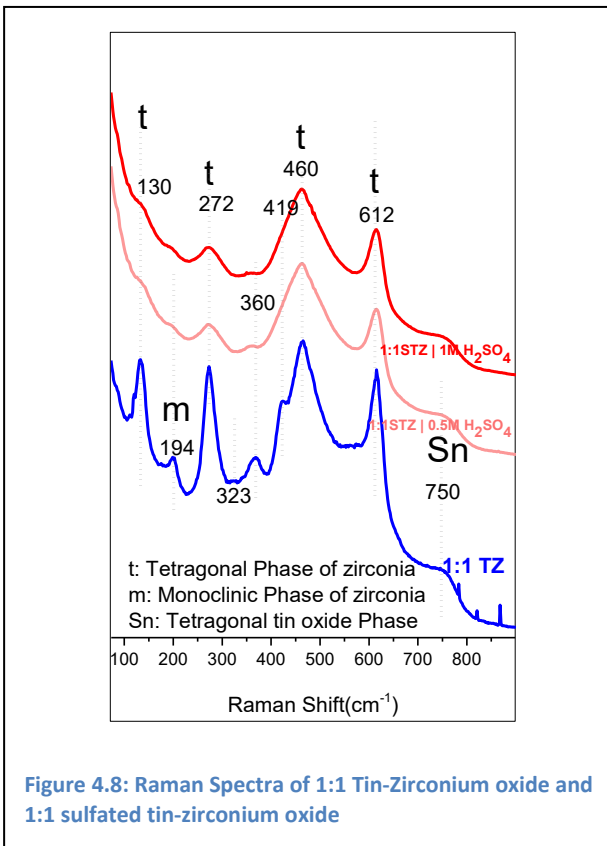
Figure 4.8: Raman Spectra of 1:1 Tin-Zirconium oxide and 1:1 sulfated tin-zirconium oxide

In order to verify this case hypothesis and examine the crystal phases of tin oxides elaborately, (as tin oxides scatter light poorly) , it is necessary to analyze the results using XRD as well.

XRD

Figure 4.9 gives the comparison of the XRD peaks of non-sulfated and sulfated mixed metal oxide crystals. The results obtained in Figure 4.1 using Raman Spectrometer corroborates with the results obtained in Figure 4.9 (A) using XRD. The XRD results show that zirconia produced is a complete match with the peak stick pattern of monoclinic zirconia. Similarly, the peaks of tetragonal phase of zirconia were a perfect

match with sulfated zirconia XRD peaks. Although, the peaks of sulfated tin oxides were broader in XRD than the peaks of non-sulfated tin oxide due to the reduction in particle size, it was found that tin oxide and sulfated tin oxide resemble to the same cassiterite mineral form of tin oxide [tetragonal phase of tin oxide]. The XRD peaks for ST were broader because smaller particle size of sulfated oxides. The crystal peak stick pattern database was obtained and matched with the XRD data using High score Plus software. The analysis using this software has helped to collect the crystallographic parameters for every individual crystal phase matched with the XRD data.

Table 4.5: Crystallographic parameters of zirconia, sulfated zirconia, tin-oxide and sulfated tin oxide

Material	Crystal system	Space group	a (A°)	b (A°)	c (A°)	A= ϒ	B
Z	Monoclinic	P21/c	5.144	5.133	5.347	90°	98.8°
SZ	Tetragonal	P42/nmc	3.6067	3.6067	5.152	90°	90°
T/ST	Tetragonal	P42/mnm	4.738	4.738	3.185	90°	90°
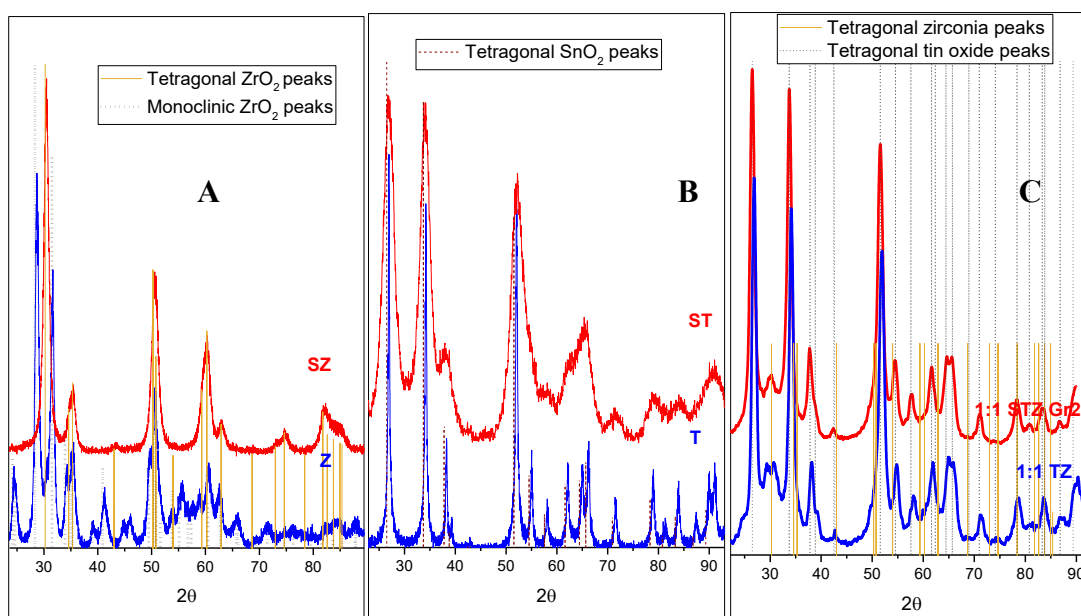
Figure 4.9:XRD of (A) sulfated zirconia and zirconia (B) sulfated tin oxide and tin oxide (C) 1:1 Sulfated tin-zirconium oxide and 1:1 tin-zirconium oxide

XRD peaks in Figure 4.9 (C) represent 1:1 STZ and TZ which emphasizes on additional information when compared to the result obtained using Raman spectrometer. The Raman spectra showed that the existence of bands of monoclinic zirconia, tetragonal zirconia and also a single band of tetragonal tin oxide. The XRD of 1:1 STZ and 1:1 TZ are very identical. The results and analysis of XRD show that majority of bands are due to tetragonal tin oxide. The only additional band, apart from tetragonal tin oxide bands, that can be seen clearly is at 30.224⁰ which correspond to the highest intensity peak of tetragonal zirconia. Rest of the peaks of tetragonal zirconia gets overshadowed by tin oxide bands. This can be due to zirconia being highly dispersed into the framework of tin oxide.
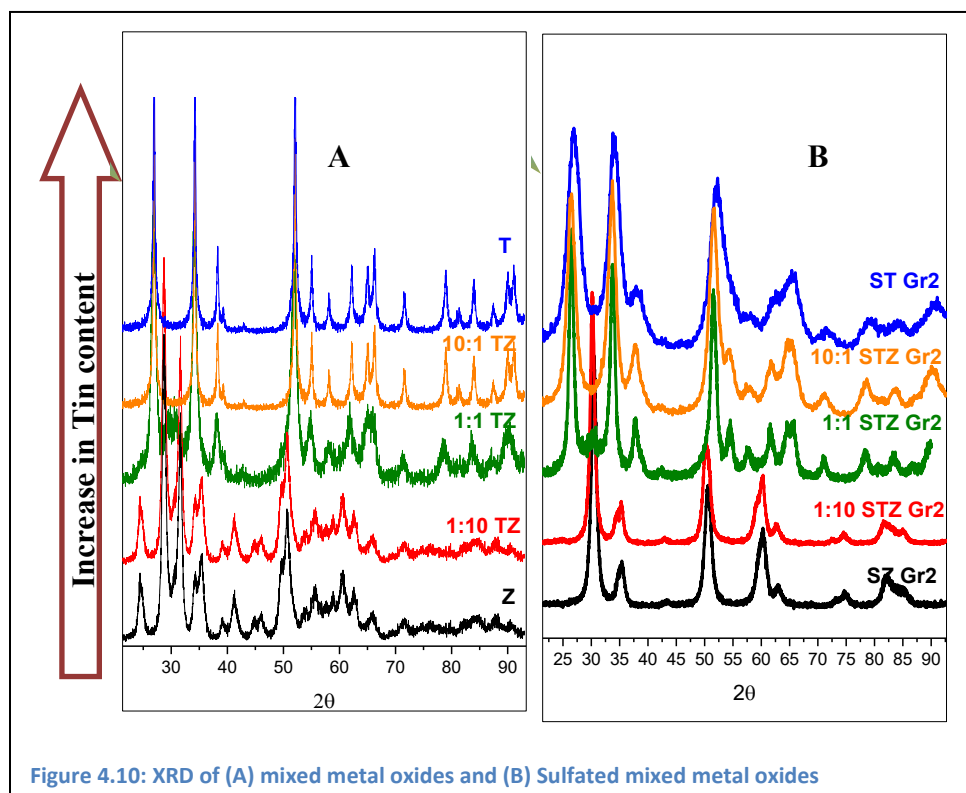
Figure 4.10: XRD of (A) mixed metal oxides and (B) Sulfated mixed metal oxides

The XRD spectra of the mixed metal oxides and sulfated mixed metal oxides are shown in Figure 4.10 It was found that the XRD peaks of zirconia and 1:10 tin-zirconia are identical. Similarly, for sulfated zirconia and 1:10 sulfated tin-zirconia mixed oxides. Even though XRD peaks of tin oxide were similar to 10:1 TZ, 10:1 STZ and ST, suggesting same crystallite phase, the peaks of 10:1 STZ and ST were broader because of sulfation. These results verify the result obtained using Raman Spectrometer.

4.3 SULFATED SPECIES

HYDROUS SULFATE SPECIES

As mentioned in the experimental section of this report, the mixed metal oxides have been impregnated with different concentrations of sulfuric acid. The Raman Spectra primarily show bands between 900 to 1450cm^{-1} for S-O and S=O symmetric and asymmetric vibrations. The Raman and the IR spectra of hydrous oxides impregnated with 1M and 0.5M sulfuric acid were collected and it was observed that the change in concentration of sulfuric acid did not affect the spectra. Hence the IR and Raman spectra for hydrous oxides impregnated only with 0.5M sulfuric acid are shown in Figure 4.11 and Figure 4.12 . All the spectra have been normalized with respect to its intensities in the range 0 to 1 and been stacked one above other. The Raman spectra of sulfated groups

shown in Figure 4.12 are focused only till 1375cm^{-1} because no vibrational bands were observed beyond the mentioned wavenumber.

The vibrational bands appearing below 1010 cm^{-1} in both IR and Raman spectra are characteristic to the components of the mixed metal hydroxide. The IR band at 996cm^{-1} for sulfated zirconium hydroxide shifts to lower wavenumbers, 966cm^{-1}, with increase in tin content. The possible explanation for the red shift could be due to replacement of zirconium atom in the solid framework with a heavier atom such as tin. Hence the band at 996 cm^{-1} can denote Zr-O-S bond whereas 966 cm^{-1} denote Sn-O-S bonds. The S-O-M bonds, where 'M' denotes support metal, could be

Figure 4.11: FTIR Spectra of (a) Hydrous Sulfated zirconium oxide, (b) Hydrous Sulfated 1:10 tin-zirconium oxide, (c) Hydrous Sulfated 1:1 tin-zirconium oxide, (d) Hydrous Sulfated 10:1 tin-zirconium oxide, (e) Hydrous Sulfated tin oxide
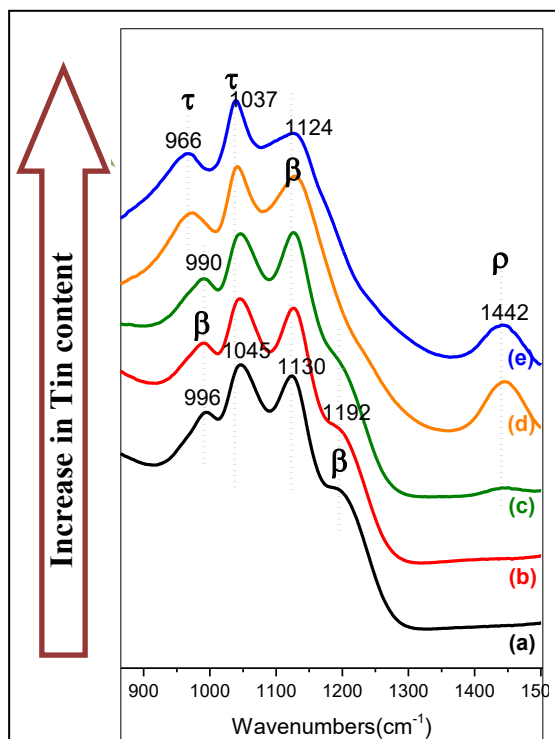
too ionic when in hydroxide form and hence difficulty arises in obtaining Raman signals at these particular vibrational bands. The bands obtained at 982cm^{-1} and 1006cm^{-1} are characteristic to the type of sulfate species. The 982cm^{-1}is assigned to the S-O symmetric stretching mode for the tridentate species and the 1004cm^{-1} is assigned to the S-O symmetric stretching mode of a bidentate species. According to the selection rules of IR and Raman spectroscopy, both the vibrational techniques act complementary to each other. The Raman spectrometer shows strong signals for symmetric stretching whereas IR shows strong signals for asymmetric stretching. With the increase in tin content, it is observed that the Raman intensity of the 982cm^{-1} increased and that of 1006cm^{-1} decreased. For 10:1 sulfated tin-zirconium hydroxide, the band at 1006cm^{-1} diminished significantly to a very low intensity because of the small amount of zirconium content and almost vanishes in the Raman spectra of sulfated tin hydroxide. The bands present at 1045cm^{-1} in IR and 1042cm^{-1} in Raman spectra can be assigned to the asymmetric stretching of the S-O bond for tridentate species. Hence it can be proposed that tin helps in developing mainly tridentate sulfated species whereas zirconium induces both bidentate and tridentate sulfate species, with majority of bidentate species in the amorphous sulfated mixed oxides. The bands appearing near 1130-1133cm^{-1} is attributed to asymmetric vibrational mode of S-O-H group which diminishes in IR and Raman intensity with increase in tin content, similarly the bands at
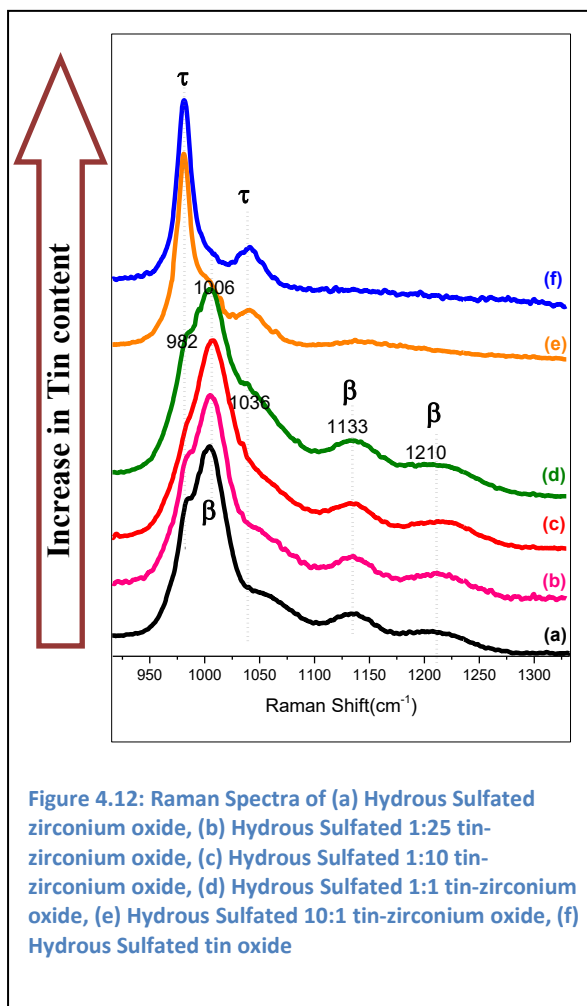

Figure 4.12: Raman Spectra of (a) Hydrous Sulfated zirconium oxide, (b) Hydrous Sulfated 1:25 tin-zirconium oxide, (c) Hydrous Sulfated 1:10 tin-zirconium oxide, (d) Hydrous Sulfated 1:1 tin-zirconium oxide, (e) Hydrous Sulfated 10:1 tin-zirconium oxide, (f) Hydrous Sulfated tin oxide

1192 cm^{-1} in IR and 1210cm^{-1} in Raman may represent S=O bond. The S=O bonds

usually appear at wavenumbers higher than 1300cm^{-1}, but due to hydration of the S=O or hydroxyl group getting attached to sulfate groups the bond order of the S=O group might decrease, which leads to appearance of this peak at lower wavenumbers. The band at 1442cm^{-1} in IR spectra can be seen rising from 1:1 STZ hydroxide with its intensity maximum for pure tin hydroxide. The reason for the appearance of vibrational bands at 1442cm-1 and 1192 cm-1 in IR specifically for tin rich hydroxides could be due to the high ionic character of the bond. The bands emerging above 1400cm^{-1} are attributed to the polysulfate species as described earlier. Therefore, it can be said that with increase in tin content the possibility of inducing polymeric sulfate species in hydroxide framework increases. It has been postulated that the metal hydroxides impregnated with sulfuric acid have sulfate groups in the solid framework's bulk phase which on calcination gets transformed to surface sulfate species.[34] The Raman technique is a bulk characterization technique and hence strong signals of sulfated group can be obtained whereas IR technique is more sensitive for analyzing surface sulfate species.

Table 4.6: Summary of band assignments of sulfate groups on hydrous mixed oxides

Material	Wavenumbers(cm-1)	Assignment
Sulfated Zirconium hydroxide	985(s)^R, 996(m),1004(vs) ^{R},1042(m) ^{R},1045(vs),	S-O
	1130(vs),1133(m) ^{R}	S-O-H
	1192(m), 1210(w-brd) ^{R}	S=O
1:1 Sulfated Tin-Zirconium Hydroxide	985(s)^R, 990(m),1004(vs) ^{R},1036(m) ^{R},1045(vs)	S-O
	1130(vs),1133(m) ^{R}	S-O
	1192(m), 1210(w-brd) ^{R},1442(vw)	S=O
Sulfated Tin hydroxide	966(m), 982(vs) ^{R},1036(m) ^{R},1037(vs)	S-O
'**R**': Band seen in Raman spectrum, '**s**': Strong Signal, '**vs**': Very strong Signal, '**m**': medium intensity signal, '**w**': weak signal, '**vw**': very weak signal, '**brd**': broad band		

Calcined sulfated mixed metal oxides

In the following section, the calcined sulfated mixed oxides are characterized at room temperature (hydrated conditions) and at dehydrated conditions. The Raman spectra and IR spectra are primarily focused on the range of wavenumbers where only bands of

sulfated group lie. After calcination the sulfate groups move to the surface of the support materials. IR is more sensitive compared to Raman spectroscopy when it comes to analysis of surface species.

It should be noted that the ambient conditions for taking FTIR and Raman spectra could be different. The Raman spectra are acquired using visible light laser at 100% intensity which can heat up the sample to some extent. Hence the spectra taken through ATR-FTIR and Raman spectrometer may present some discrepancies. The degree of hydration could affect the spectra more in the case of FTIR.

Sulfated Zirconia

Mortera et.al. reported that the 3 asymmetric modes 1215, 1150 and 1085 are observed in anhydrous inorganic sulfates which also have C_{2v} symmetry.[35] Removal of water brings the sulfate group in direct contact with metal and thus increasing the covalent character of the band. The IR band at 1218cm^{-1} for sulfated zirconia collected at room temperature can be assigned inorganic sulfate group. This can be justified by comparing the band with Raman spectra. Inorganic sulfates have ionic character. The band at 1218 cm^{-1} is missing in Raman spectra collected; this is due to the too ionic character of the bond to be visible through Raman spectrometer. The broad IR band starting from 1218cm-1 engulfs band existing at 1280-1300. This band present in IR and Raman spectra is assigned to the hydrated asymmetric stretching of S=O group for chelating bidentate sulfate species. Similarly the band at 1135-1140 can be assigned to hydrated S-O asymmetric stretching mode of bidentate sulfate species[31].
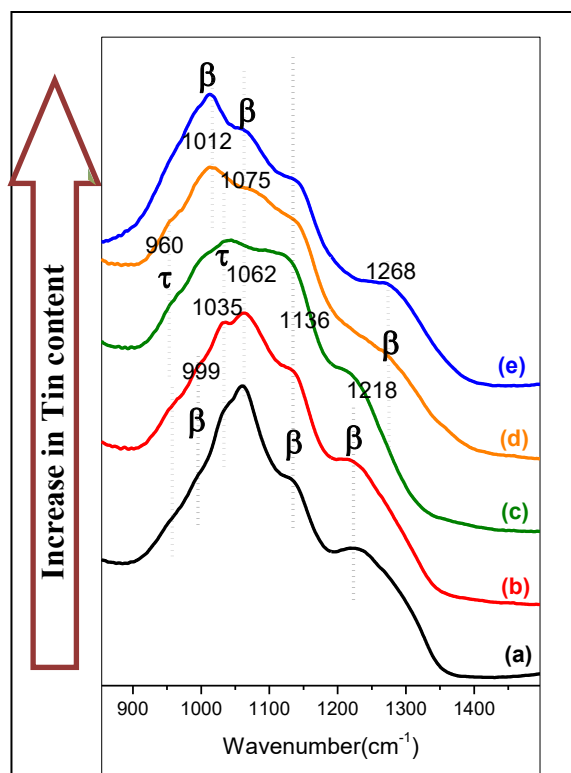

Figure 4.13: FTIR Spectra of (a) Sulfated zirconium oxide, (b) Sulfated 1:10 tin-zirconium oxide, (c) Sulfated 1:1 tin-zirconium oxide, (d) Sulfated 10:1 tin-zirconium oxide, (e) Sulfated tin oxide

The intensity of this band drops when the sample is dehydrated. The wavenumber range from 900 to 1100 presents many vibrational bands in the IR and Raman spectra underscoring the difficulty of the interpretation. Interpreting the bands appearing from 1100 to 1400 is easier. Consider the FTIR spectrum of sulfated Zirconia taken at room temperature (See Figure 4.13). The strongest band being $1062cm^{-1}$, is assigned to bidentate sulfate complex species[32], the same band can be seen around $1070cm^{-1}$ in Raman. On dehydration it can be seen that this band red shifts to $1012\ cm^{-1}$, which can again be assigned to bidentate sulfate configuration (Figure 4.15).

Now consider the IR band at $1081cm^{-1}$ for sulfated zirconia at $200^{o}C$: this band cannot be due to the inorganic character of the bond. This band is assigned to another sulfate species. Bensitel and coworkers[36] assigned this peak to polymeric sulfate group which is

in complete agreement with the ambient conditions. Collecting Raman spectra for sulfated zirconia at high temperature with 532nm was challenging because of the interference in the spectra due to fluorescence. Avoiding fluorescence in the case of sulfated zirconia was not possible, therefore only the high intensity bands visible at 1000, 1035 and $1400cm^{-1}$ can be trusted (See Figure 4.16). Hence the existence of band at $1081cm^{-1}$ cannot be rightfully justified. The sharp band seen at 1400 cm-1 is possibly due to asymmetric stretching of S=O bond for tridentate or polymeric species.

The Raman and IR band seen at $1035cm^{-1}$ is assigned to S-O stretching of tridentate sulfate species. This band
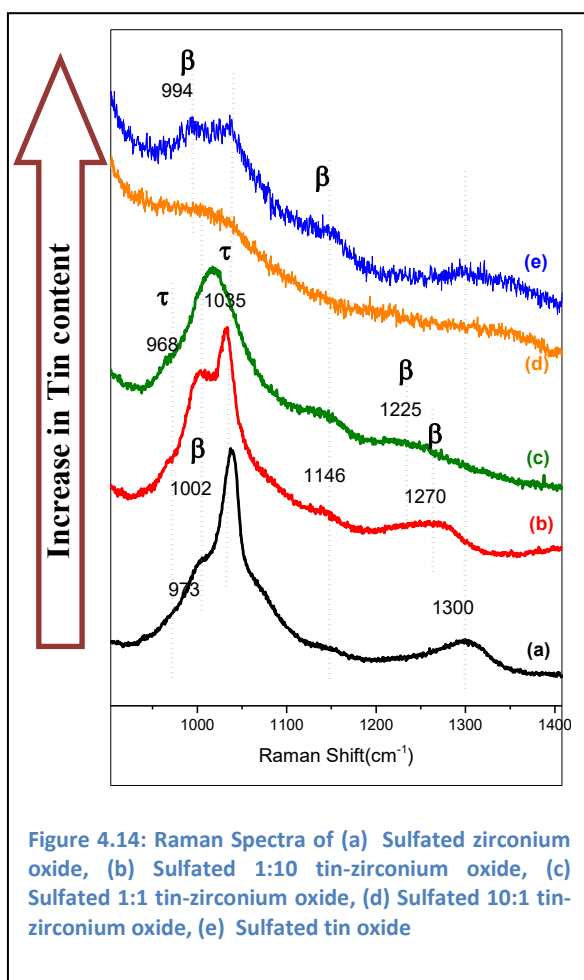

Figure 4.14: Raman Spectra of (a) Sulfated zirconium oxide, (b) Sulfated 1:10 tin-zirconium oxide, (c) Sulfated 1:1 tin-zirconium oxide, (d) Sulfated 10:1 tin-zirconium oxide, (e) Sulfated tin oxide

remains unaffected even after treating the material to a high temperature. Hence this

proves the theory put forth by Bensitel that the tridentate species are free from any kind of hydrogenosulfates.

The Raman band appearing at 1002cm-1 at room temperature remains almost at the same position after treating the sample at high temperature. This band can be assigned to symmetric S-O stretching mode for bidentate species.[31]

The lower wavenumber bands around 960-975 for Raman and IR is assigned to S-O tridentate sulfate species. The Raman and IR spectra obtained for 1:10 sulfated tin-zirconium is almost the same except a minute rise in intensity around 960-975. This reflects the increase in S-O-Sn bond.

1:1 Sulfated Tin-Zirconium oxide

With further increase in tin content i.e. the Raman and spectra for 1:1 STZ changes significantly. The main difference is of appearance of only one peak at 1019 cm$^-$^{1} (see Figure 4.14 and Figure 4.16), instead of doublet at 1000 and 1035cm^{-1}, which remains unchanged even after dehydration. This band is also assigned to S-O stretching mode of tridentate species. The difference in the spectra of sulfated zirconia and 1:1 STZ arises due to morphological differences in crystal phases of these samples. The Raman band at 1225cm^{-1} at room temperature for 1:1 STZ can be assigned to the bridged bidentate sulfate species as the probability of sulfate species anchoring to both metals, tin and zirconium, is more than anchoring to just one of the components. This assignment can be

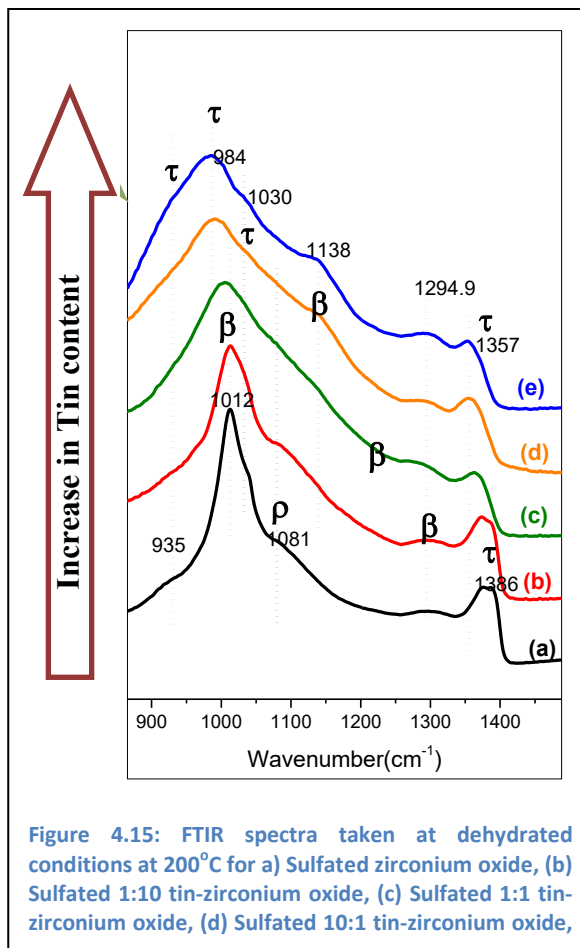Figure 4.15: FTIR spectra taken at dehydrated conditions at 200°C for a) Sulfated zirconium oxide, (b) Sulfated 1:10 tin-zirconium oxide, (c) Sulfated 1:1 tin-zirconium oxide, (d) Sulfated 10:1 tin-zirconium oxide,

conceptually justified by referring to section 1.7. The Raman spectrum for 1:1 STZ collected using the HVC at 25°C after dehydrating at 500°C shows bands at 1019, 1200,

1300 and 1391cm^{-1}. The broad bands at 1200 and 1300cm^{-1} is due to hydrated S=O bidentate sulfate species. These 2 bands are missing from the Raman spectra taken at high temperatures (not included in this report). The band at 1391 cm^{-1} arises due to asymmetric stretching of S=O bond in tridentate sulfate species. Hasse and Sauer[39] predicted that bidentate species are not thermodynamically stable at high temperatures in sulfated zirconia and transforms to tridentate species. Thus the Raman spectrum for 1:1 STZ after dehydration confirms the above theory. The IR spectrum for 1:1 STZ is broad and hence difficult to be elucidated. Nevertheless small bumps at 960, 1035, 1130,1218 cm^{-1} can be seen which is assigned to same configurations or bonds as that in sulfated zirconia.

Sulfated Tin oxide

Now consider Sulfated tin oxide sample, the Raman bands are not clear as tin oxide does not scatter light well hence the resolution is very low. The Raman spectrum of tin oxide and sulfated tin oxide in the 900 to 1400 region at room temperature is almost the same. But as the IR is more sensitive when it comes to surface species, bands for sulfate group can be seen in sulfated tin oxide which didn't exist in pure tin oxide. Hence it would be wrong to assume that the bands due to sulfate groups don't exist for sulfated tin oxide if only Raman spectrum at room temperature is considered. Also the Raman bands are clearly visible at 1000, 1137, 1300, 1356 cm^{-1} for dehydrated sulfated tin oxide. The IR

Figure 4.16: Raman spectra taken at 500°C for (a) Sulfated Zirconia and Raman Spectra taken at 25°C after dehydrating at 500°C for (b) Sulfated 1:1 tin-zirconium oxide, (c) Sulfated tin oxide

band at 1012cm^{-1} at room temperature (See Figure 4.13) can be assigned to hydrated S-O stretching mode of bidentate species which gets transformed to tridentate sulfate species
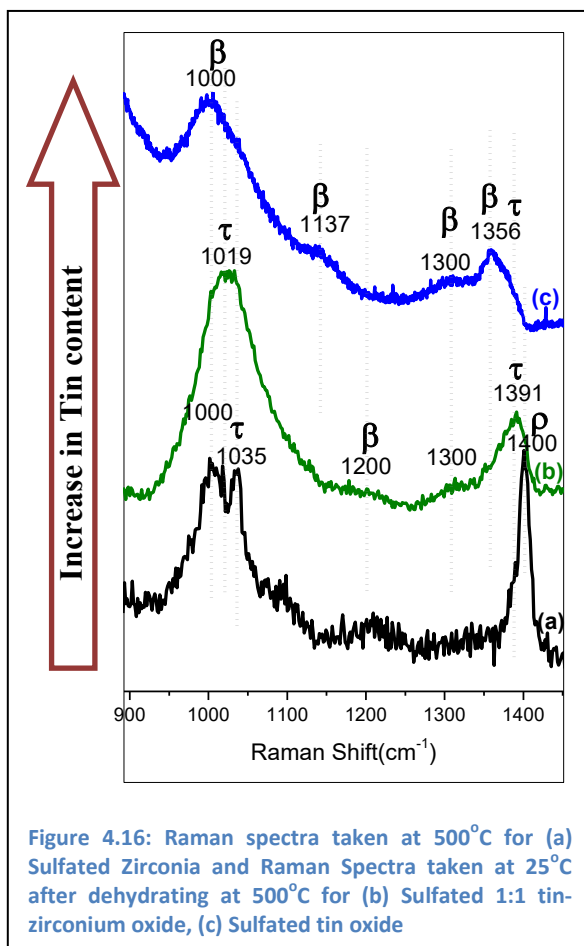
as the band shifts to 984cm^{-1}. The other IR bands at room temperature which appear at 1075, 1136, 1268 is assigned to the assymetric stretching of S-O and S=O bonds in bidentate species.[32] The IR bands collected at 200°C have vibrational bands at 1030, 1138, 1300 and 1357. The 1030 cm-1 band can be seen as a weak band in Raman spectra for dehydrated sulfated tin oxide sample as well. As explained for sulfated zirconia, 1030 cm-1 band can also be assigned to S-O stretching in tridentate species. The Raman spectrum at dehydrated conditions shows a strong band at 1000cm^{-1} which denotes bidentate sulfate species, whereas 1137 and 1300 cm^{-1} is assigned to hydrated S-O and S=O bidentate sulfate species. The wide band at 1356 cm-1 can be a combination of asymmetric S=O stretching mode of bidentate and tridentate sulfate species.

4.4   FUTURE WORK

Alkylation of phenol

The quantitative analysis of products and reactants through GC-MS showed that the catalytic activity of 1:1 Sulfated Tin- Zirconium oxide catalyst for catalytic phenol conversions was higher than the conversions   obtained with hierarchical

Figure 4.17: Summary of alkylation of phenol reaction

ZSM-5 zeolite[59], sulfated Fe$_2$O$_3$–TiO$_2$[60] whereas for 1:10 Sulfated Tin- Zirconium oxide the catalytic activity was poor. The result can be seen in Table 4.7. The alkylation reactions were run only once for both of these catalysts in order to check its reactivity. The amount of olefins produced can be controlled by regulating the ratio of alkylating reagent to phenol. Hence by running the reaction at optimized parameters the activity of the catalyst can be improved. Also by impregnating these catalysts with transition metals like tungsten and molybdenum, the reactivity and selectivity could be improved.

Table 4.7: Catalytic activity results for butylation of phenol

Catalyst	t-butanol conversion	Phenol conversion	Products selectivity (%) Alkylated	Olefins
1:1 STZ	100	80	66	34
10:1 STZ	100	10	91	9

The catalyst was separated from the reaction mixture and it was observed that the catalyst had turned black. In order to drive out the organic matter from the samples, the 1:1 STZ and 1:10 STZ were calcined at 600°C for 3 hours. The regenerated catalyst regained the
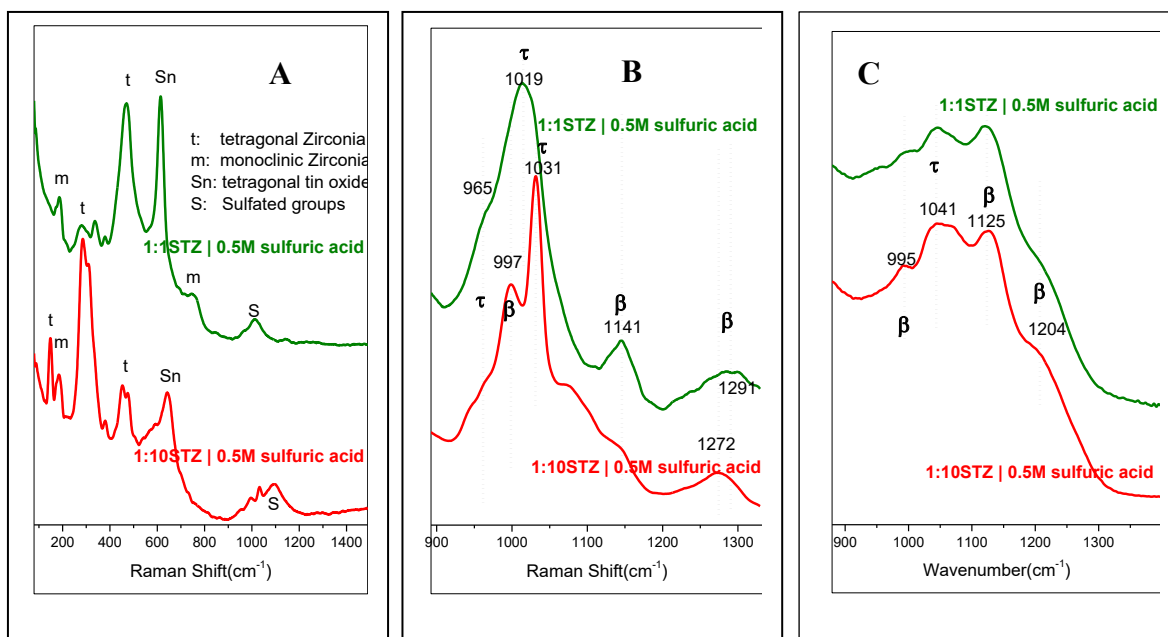
Figure 4.18: (A) Raman Spectra of regenerated 1:1 STZ and 1:10 STZ, (B) Raman spectra of regenerated 1:1 STZ and 1:10 STZ from 900 to 1350cm^{-1}, (C) FTIR Spectra of regenerated 1:1 STZ and 1:10 STZ

same color. The Raman and IR spectra were collected at room temperature for the regenerated catalyst and they were almost identical to the spectra obtained before the alkylation reaction (see Figure 4.18). This experiment showed that the catalyst synthesized can be regenerated and the sulfated species remain intact, making it a stable catalyst.

5   CONCLUSION

Vibrational spectroscopy was employed to study the crystalline phases of mixed metal oxides and also to elucidate the structural configuration of surface sulfate species formed on the support oxides. The Raman and IR spectra of sulfate groups for hydrous sulfated mixed metal oxides and calcined sulfated mixed metal oxides reveal that the sulfate species formed majorly in hydrated conditions is bidentate sulfate species. The intensity of bands assigned to bidentate surface species drop for sulfated zirconia and 1:1 STZ as a function of temperature. The surface sulfate species embedded on tin oxide at higher temperatures manifested as a combination of bidentate and tridentate species. In the case of sulfated zirconia all 3 types of postulated structures exist. Polymeric and tridentate sulfate species were majorly formed on sulfate zirconia. It can also be concluded that only sulfated zirconia or zirconia rich sulfated mixed metal oxides could induce polymeric sulfate groups on its support at dehydrated conditions. It was found that metastable tetragonal phase of zirconia can be stabilized by coprecipitating zirconium hydroxide with tin hydroxide at equimolar proportions, even without sulfate group impregnation. The mixed metal oxide formed, exists as 2 different component oxides and doesn't form a single phase of Zr-Sn. The Raman spectra and XRD of 1:1 STZ and 1:1 TZ are not different and hence it can be concluded that sulfate group impregnation doesn't change the crystalline phase as it does for zirconia. It would not be wrong to state that the sulfate structure formed on 1:1 STZ at dehydrated conditions only induces tridentate sulfate species. This proves the project's hypothesis that by modulating the tin content in zirconium oxide framework the morphology of the crystalline phase can be changed which in turn helps to tune the surface sulfate species anchored on to the support. On the later part of this research work, the catalytic activity and regeneration ability of 1:1STZ and 1:10 STZ was investigated. The results proved that 1:1 STZ is catalytically active for butylation of phenol reaction and also to be a stable catalyst.

6   REFERENCES

1.   Corma, A., Inorganic Solid Acids and Their Use in Acid-Catalyzed Hydrocarbon Reactions. *Chem Rev* **1995**, *95*, 559-614.

2.   Cseri, T.; Bekassy, S.; Figeuras, F.; Cseke, E.; deMenorval, L. C.; Dutartre, R., Characterization of Clay-Based K Catalysts and Their Application in Friedel-Crafts Alkylation of Aromatics. *Applied Catalysis A:General* **1995**, *132*, 141-155.

3.   Courty, P.; Marcilly, C., *Preparation of Catalysts Iii*; Elsevier; p.485.: Amsterdam, 1983.

4.   Jin, T.; Yamaguchi, T.; Tanabe, K., Mechanism of Acidity Generation on Sulfur-Promoted Metal-Oxides. *J Phys Chem-Us* **1986**, *90*, 4794-4796.

5.   Arataa, K.; Matsuhashia, H.; Hinob, M.; Nakamura, H., Synthesis of Solid Superacids and Their Activities for Reactions of Alkanes. *Catalysis Today* **2003**, *81*, 17-30.

6.   Srinivasan, R.; Davis, B. H., Zirconia: A Review of a Super Ceramic. *Materials Synthesis and Characterization* **1997**, 147-188.

7.   Clearfield, A.; Vaughan, P., *Acta Crystallographica* **1956**, 555.

8.   Davis, B. H., Effect of Ph on Crystal Phase of Zro2 Precipitated from Solution and Calcined at 600-Degrees-C. *J Am Ceram Soc* **1984**, *67*, C168-C169.

9.   Srinivasan, R.; Davis, B. H., Influence of Zirconium Salt Precursors on the Crystal-Structures of Zirconia. *Catal Lett* **1992**, *14*, 165-170.

10.   Clearfield, A., *Reviews of Pure and Applied Chemistry,* **1964**, *14*, 91.

11.   McCullough, J.; Trueblood, K., *Acta Crystallographica* **1959**, *12*, 507.

12.   Li, W. J.; Shi, E. W.; Zhong, W. Z.; Yin, Z. W., Growth Mechanism and Growth Habit of Oxide Crystals. *J Cryst Growth* **1999**, *203*, 186-196.

13.   Jung, K. T.; Bell, A. T., Effects of Zirconia Phase on the Synthesis of Methanol over Zirconia-Supported Copper. *Catal Lett* **2002**, *80*, 63-68.

14.   Garvie, R. C., Thermodynamic Analysis of the Tetragonal to Monoclinic Transformation in a Constrained Zirconia Microcrystal. *Journal of Material Science* **1985**, *20*, 3479-3486.

15.   Norman, C. J.; Goulding, P. A.; Mcalpine, I., Role of Anions in the Surface-Area Stabilization of Zirconia. *Catal Today* **1994**, *20*, 313-322.

16.   Arata, K.; Hino, M., *Hyomen* **1981**, *19*, 75.

17.   W. Stichert, F. S., S. Kuba, H. Knozinger, Monoclinic and Tetragonal High Surface Area Sulfated Zirconias in Butane Isomerization: Co Adsorption and Catalytic Results. *Journal of Catalysis* **2001**, *198*, 277-285.

18.   Y. Zhao, K. T., H.L. Wan, Effect of Zirconia Phase on the Reduction Behaviour of Highly Dispersed Zirconia-Supported Copper Oxide. *Catalysis Communications* **2004**, *5*, 249-252.

19.   Batzill, M.; Diebold, U., The Surface and Materials Science of Tin Oxide. *Progress in Surface Science* **2005**, *79*, 47–154.

20.   Matsuhashi, H.; Hino, M.; Arata, K., Synthesis of the Solid Superacid of Sno2 Treated with Sulfate Ion. *Acid-Base Catalysis* **1989**, 357-362.

21.   Zhou, L.; Xu, B.; Hua, W.; Yue, Y.; Gao, Z., Sulfated Tin Oxide: An Efficient Catalyst for Alkylation of Hydroquinone. *Catalysis Communication* **2008**, *9*, 2274–2277.

22.   Hua, W. M.; Goeppert, A.; Sommer, J., H/D Exchange and Isomerization of Small Alkanes over Unpromoted and Al2o3-Promoted So42-/Zro2 Catalysts. *Journal of Catalysis* **2001**, *197*, 406-413.

23.   Rosenberg, D.; Coloma, F.; Anderson, J., Modification of the Acid Properties of Silica-Zirconia Aerogels by in Situ and Ex Situ Sulfation. *Journal of Catalysis* **2002**, *210*, 218-228.

24.   Xia, Y.; Hua, W.; Gao, Z., A New Catalyst for N-Butane Isomerization: Persulfate-Modified Al2o3-Zro2. *Applied Catalysis A: General* **1999**, *185*, 293-300.

25.   Reddy, B.; Sreekanth, P.; Yamada, Y.; Xu, X.; Kobayashi, T., Surface Characterization of Sulfate, Molybdate, and Tungstate Promoted Tio2-Zro2 Solid Acid Catalysts by Xps and Other Techniques. *APPLIED CATALYSIS A-GENERAL* **2002**, *228*, 269-278.

26.   Tanabe, K.; Sumiyoshi, T.; Shibata, K.; Kiyoura, T.; Kitagawa, J., New Hypothesis Regarding the Surface Acidity of Binary Metal Oxides. *Bulletin of Chemical Society* **1974**, *47*, 1064-1066.

27.   Alhassan, F. H.; Rashid, U.; Taufiq-Yap, Y. H., Synthesis of Waste Cooking Oil-Based Biodiesel Via Effectual Recyclable Bi-Functional Fe2o3-Mno-So42-/Zro2 Nanoparticle Solid Catalyst. *Fuel* **2015**, *142*, 38-45.

28.   Reddy, B. M.; Reddy, G. K.; Rao, K. N.; Katta, L., Influence of Alumina and Titania on the Structure and Catalytic Properties of Sulfated Zirconia: Beckmann Rearrangement. *J Mol Catal a-Chem* **2009**, *306*, 62-68.

29.   Chen, W. H.; Ko, H. H.; Sakthivel, A.; Huang, S. J.; Liu, S. H.; Lo, A. Y.; Tsai, T. C.; Liu, S. B., A Solid-State Nmr, Ft-Ir and Tpd Study on Acid Properties of Sulfated and Metal-Promoted Zirconia: Influence of Promoter and Sulfation Treatment. *Catal Today* **2006**, *116*, 111-120.

30.   Arata, K.; Hino, M., Solid Catalyst Treated with Anion .18. Benzoylation of Toluene with Benzoyl Chloride and Benzoic Anhydride Catalyzed by Solid Superacid of Sulfate-Supported Alumina. *Appl Catal* **1990**, *59*, 197-204.

31.   Yamaguchi, T.; Jin, T.; Tanabe, K., Structure of Acid Sites on Sulfur-Promoted Iron-Oxide. *J Phys Chem-Us* **1986**, *90*, 3148-3152.

32.   Nakamoto, K., *Infrared and Raman Spectra of Inorganic and Coordination Compounds,*; 3rd Edition, Wiley, p.241: New York, 1978.

33.   Hug, S. J., In Situ Fourier Transform Infrared Measurements of Sulfate Adsorption on Hematite in Aqueous Solutions. *J. Colloid Interface Sci.* **1997**, *188*, 415-422.

34.   Ward, D. A.; Ko, E. I., One-Step Synthesis and Characterization of Zirconia-Sulfate Aerogels as Solid Superacids. *J Catal* **1994**, *150*, 18-33.

35.   Morterra, C.; Cerrato, G.; Pinna, F.; Signoretto, M.; Strukul, G., On the Acid-Catalyzed Isomerization of Light Paraffins over a Zro2/So4 System - the Effect of Hydration. *J Catal* **1994**, *149*, 181-188.

36.   Bensitel, M.; Saur, O.; Lavalley, J. C.; Morrow, B. A., An Infrared Study of Sulfated Zirconia. *Mater Chem Phys* **1988**, *19*, 147-156.

37.   Waqif, M.; Bachelier, J.; Saur, O.; Lavalley, J. C., Acidic Properties and Stability of Sulfate-Promoted Metal-Oxides. *Journal of Molecular Catalysis* **1992**, *72*, 127-138.

38.   Riemer, T.; Spielbauer, D.; Hunger, M.; Mekhemer, G. A. H.; Knozinger, H., Superacid Properties of Sulfated Zirconia as Measured by Raman and H-1 Mbs Nmr-Spectroscopy. *J Chem Soc Chem Comm* **1994**, 1181-1182.

39.   Haase, F.; Sauer, J., The Surface Structure of Sulfated Zirconia: Periodic Ab Initio Study of Sulfuric Acid Adsorbed on Zro2(101) and Zro2(001). *J Am Chem Soc* **1998**, *120*, 13503-13512.

40.   White, R. L.; Sikabwe, E. C.; Coelho, M. A.; Resasco, D. E., Potential Role of Penta-Coordinated Sulfur in the Acid Site Structure of Sulfated Zirconia. *J Catal* **1995**, *157*, 755-758.

41.   Modrogan, E.; Valkenberg, M.; Hoelderich, W., Phenol Alkylation with Isobutene - Influence of Heterogeneous Lewis and/or Bronsted Acid Sites. *Journal of Catalysis* **2009**, *261*, 177-187.

42.   Mitra, A. Doctoral dissertation: IIT-Bombay, 1997.

43.   Anand, R.; Maheswari, R.; Gore, K. U.; Tope, B. B., Tertiary Butylation of Phenol over Hy and Dealuminated Hy Zeolites. *J Mol Catal a-Chem* **2003**, *193*, 251-257.

44.   Sakthivel, A.; Saritha, N.; Selvam, P., Vapour Phase Tertiary Butylation of Phenol over Sulfated Zirconia Catalyst. *Catal Lett* **2001**, *72*, 225-228.

45.   Ravi, V.; Venugopalarao, N.; Sripad, R. K.; Mujeeb, K.; Abdulrahman, A.; Syed, F. A., Sulfated Tin Oxide (Sto) – Structural Properties and Application in Catalysis: A Review. *Arabian Journal of Chemistry, Vol 9, Iss 4, Pp 550-573 (2016)* **2016**, 550.

46.   Ahmed, A. I.; El-Hakam, S. A.; Khder, A. S.; Abo El-Yazeed, W. S., Nanostructure Sulfated Tin Oxide as an Efficient Catalyst for the Preparation of 7-Hydroxy-4-Methyl Coumarin by Pechmann Condensation Reaction. *Journal of Molecular Catalysis. A, Chemical* **2013**, *366*, 99-108.

47.   Wang, G.-W.; Hattori, H.; Tanabe, K., Acid-Base and Catalytic Properties of Zro//2-Sno//2. *B Chem Soc Jpn* **1983**, *56*, 2407-2410.

48.   Patel, A.; Coudurier, G.; Essayem, N.; Védrine, J. C., Effect of the Addition of Sn to Zirconia on the Acidic Properties of the Sulfated Mixed Oxide. *Journal of the Chemical Society - Faraday Transactions* **1997**, *93*, 347-353.

49.   Stichert, W.; Schüth, F.; Kuba, S.; Knözinger, H., Regular Article: Monoclinic and Tetragonal High Surface Area Sulfated Zirconias in Butane Isomerization: Co Adsorption and Catalytic Results. *J Catal* **2001**, *198*, 277-285.

50.   Burkov, K. A.; Kozhevnikova, G. V.; Lilich, L. S.; Myund, L. A., Vibrational-Spectra of a Zirconium(Iv) Tetramerous Hydroxocomplex. *Zh Neorg Khim+* **1982**, *27*, 1427-1431.

51.   Kozhevnikova, G. V.; Myund, L. A.; Burkov, K. A., Raman-Spectra of Zirconium Oxychloride Crystalline Hydrate and Solutions. *Inorg Mater+* **1988**, *24*, 383-386.

52.   Tosan, J. L.; Durand, B.; Roubin, M.; Chassagneux, F.; Mosoni, L.; Bertin, F.; Moraweck, B., Ph-Metric and Raman Investigations of Zirconium Aquoeus Solutions and Gels Submitted to a Reflux. *Journal of Non-Crystalline Solids* **1993**, *1993*, 167-176.

53.   Southon, P. D.; Bartlett, J. R.; Woolfrey, J. L.; Ben-Nissan, B., Formation and Characterization of an Aqueous Zirconium Hydroxide Colloid. *Chem Mater* **2002**, *14*, 4313-4319.

54.   Ishigame, M.; Sakurai, T., Temperature Dependence of the Raman Spectra of Zro2. *Journal of the American Ceramic Society* **1977**, *60*, 367.

55.   Noda, L. K.; N.S, G.; Borba, S. M.; J.A, S., Raman Spectroscopy and Thermal Analysis of Sulfated Zro2 Prepared by Two Synthesis Routes. *Vibrational Spectroscopy* **2007**, *44*, 101-107.

56.   M. Ishigame, T. S., Temperature Dependence of the Raman Spectra of Zro2. *Journal of the American Ceramic Society* **1977**, *60*, 367.

57.   Naumenko, A. P.; Berezovska, N. I.; Biliy, M. M.; O.V, S., Vibrational Analysis and Raman Spectra of Tetragonal Zirconia. *Physics and Chemistry of Solid State* **2008**, *9*, 121-125.

58.   Dieguez, A.; Romano-Rodriguez, A.; Vila, A.; J.R., M., The Complete Raman Spectrum of Nanometric Sno2 Particles. *Journal of Applied Physics* **2001**, *90*, 1550-1557.

59.   Song, Y. D.; Hua, Z. L.; Zhu, Y.; Zhou, J.; Zhou, X. X.; Liu, Z. C.; Shi, J. L., Solvent-Free Liquid Phase Tert-Butylation of Phenol over Hierarchical Zsm-5 Zeolites for the Efficient Production of 2,4-Ditert-Butylphenol. *J. Mater. Chem.* **2012**, *22*, 3327-3329.

60.   Raj, K. J. A.; Prakash, M. G.; Viswanathan, B., Selective Ortho Butylation of Phenol over Sulfated Fe2o3-Tio2. *Catal Sci Technol* **2011**, *1*, 1182-1188.